



Article

Edge Race-Tracking during Film-Sealed Compression Resin Transfer Molding

Mario Vollmer ^{1,*}, Swen Zaremba ¹, Pierre Mertiny ²  and Klaus Drechsler ¹

¹ Chair of Carbon Composites, TUM School of Engineering and Design, Technical University of Munich, Boltzmannstrasse 15, 85748 Garching bei München, Germany; Zaremba@tum.de (S.Z.); Klaus.Drechsler@tum.de (K.D.)

² Advanced Composite Materials Engineering Group, Department of Mechanical Engineering, University of Alberta, 9211-116 Street NW, Edmonton, AB T6G 2H5, Canada; pmertiny@ualberta.ca

* Correspondence: Mario.Vollmer@tum.de; Tel.: +49-89-289-15788

Abstract: Edge race-tracking is a frequently reported issue during resin transfer molding. It is caused by highly permeable channels and areas between the preform edge and cavity, which can significantly change the preform impregnation pattern. To date, information is scarce on the effect of edge race-tracking in compression resin transfer molding (CRTM). To close this gap, laboratory equipment was developed to study the CRTM preform impregnation via flow visualization experiments. The preform was thereby encapsulated in thin thermoplastic films sealing its impregnation. Film-sealed compression resin transfer molding (FS-CRTM) experiments of preforms with a small geometrical aspect ratio showed fast filling of the injection gap and a subsequent through-thickness preform impregnation. Creating an edge race-tracking channel, an additional lateral in-plane flow from the channel towards the preform center was observed, initiating soon after the injection started and caused by the spatial connection between the injection gap and the race-tracking channel. To diminish edge race-tracking, a passive flow control strategy was implemented via a split design of the upper tool to spatially isolate the injection gap from the channel and to pre-compact the preform edge. A delayed and reduced lateral race-tracking flow was observed, showing that the passive flow control strategy increases the process robustness of FS-CRTM regarding edge race-tracking effects.

Keywords: edge race-tracking; film-sealed compression resin transfer molding; flow visualization; flow control; passive process control strategy



Citation: Vollmer, M.; Zaremba, S.; Mertiny, P.; Drechsler, K. Edge Race-Tracking during Film-Sealed Compression Resin Transfer Molding. *J. Compos. Sci.* **2021**, *5*, 195. <https://doi.org/10.3390/jcs5080195>

Academic Editor: Francesco Tornabene

Received: 21 June 2021
Accepted: 8 July 2021
Published: 21 July 2021

Publisher's Note: MDPI stays neutral with regard to jurisdictional claims in published maps and institutional affiliations.



Copyright: © 2021 by the authors. Licensee MDPI, Basel, Switzerland. This article is an open access article distributed under the terms and conditions of the Creative Commons Attribution (CC BY) license (<https://creativecommons.org/licenses/by/4.0/>).

1. Introduction

The excellent weight-specific mechanical properties of fiber reinforced plastic (FRP) materials hold high potential for the transport industry to develop lighter and more efficient solutions. Ecologically, lighter designs help to reduce CO₂ emissions. Economically, they allow for increased payload and the expanded driving range of vehicles [1,2]. In the automotive industry, manufacturing of FRP components via closed mold liquid composite molding processes has been shown to meet the industry's strict requirements of high-quality structural parts at reasonable production costs. Specifically, the compression resin transfer molding (CRTM) process is used for medium to large volume serial production of FRP parts [3–5].

During the CRTM production cycle, a dry reinforcement structure in the shape of the final part, commonly referred to as the preform, is manufactured and placed inside the cavity of a rigid mold. A polymeric resin is injected into the cavity to fully impregnate the preform. After curing of the resin, the final FRP part can be removed from the mold. The key characteristic of the CRTM process is the integration of active tool movement to control the process. Thus, the resistance to resin flow inside the cavity can be adjusted during the preform impregnation to significantly minimize production cycle times. In the literature, the preform impregnation during CRTM is divided into two subsequent

process phases: the injection phase and the compression phase. In the injection phase a defined amount of resin is injected into the cavity, partially impregnating the preform. In the compression phase, the tool is closed to compact the preform to the final part thickness and distribute the resin in order to fully impregnate the preform. Prior to resin injection, the tool is either closed to be slightly in contact with the preform to enable an injection into a preform with high permeability, or the tool can be kept open further to realize an injection gap between the preform top surface and the upper tool cavity [6]. The injection gap in the latter process setting acts as a resin distribution space of low flow resistance, which for preforms with a small geometrical aspect ratio (length/width versus height) of 10–100, causes a predominant in-plane filling of the injection gap and a subsequent through-thickness preform impregnation [7,8]. For shell structures with a larger geometrical aspect ratio of 100–1000, the permeability of the gap was reported in [8,9] to be not low enough to fully distribute the resin above the preform before the upper tool is in contact with the preform. Even though the CRTM process variant with injection gap involves a more complex three-dimensional preform impregnation pattern, it also provides the highest potential to minimize injection pressure and cycle times.

In [10], the conventional CRTM process is enhanced by using thin thermoplastic films to seal the preform impregnation, enabling a seal-free tool design. The principal steps of the so-called film-sealed compression resin transfer molding (FS-CRTM) process are illustrated in Figure 1. The preform is encapsulated within two layers of film and sealed by welding the film layers to each other, which allows for evacuation prior to placing the film-sealed preform package inside the mold. Due to the advantage of the tool not needing to be sealed, more complex tool designs can be realized using, for example, slider technology to enable undercuts or to create localized injection gaps only covering a section of the preform surface (see Figure 1). During the injection phase, the film is penetrated, and the resin is injected into the film-sealed preform package. Due to the elastic behavior of the film, it can lift off the preform and expand to allow the resin to be easily distributed inside the injection gap. During the subsequent compression phase, the tool is closed further, distributing the resin to fill the complete preform. Since the film acts as a barrier layer between the preform impregnation space and the cavity wall, the film seals the tool and, additionally, enables a release agent-free FRP production. While the film is suggested in [10] to be solely used as a process aid material, which is intended to be removed after the part is cured, it can also be designed to co-cure with the resin and remain on the part as a functional layer to enable, for example, a weldable part surface or an integration of sensors [11].

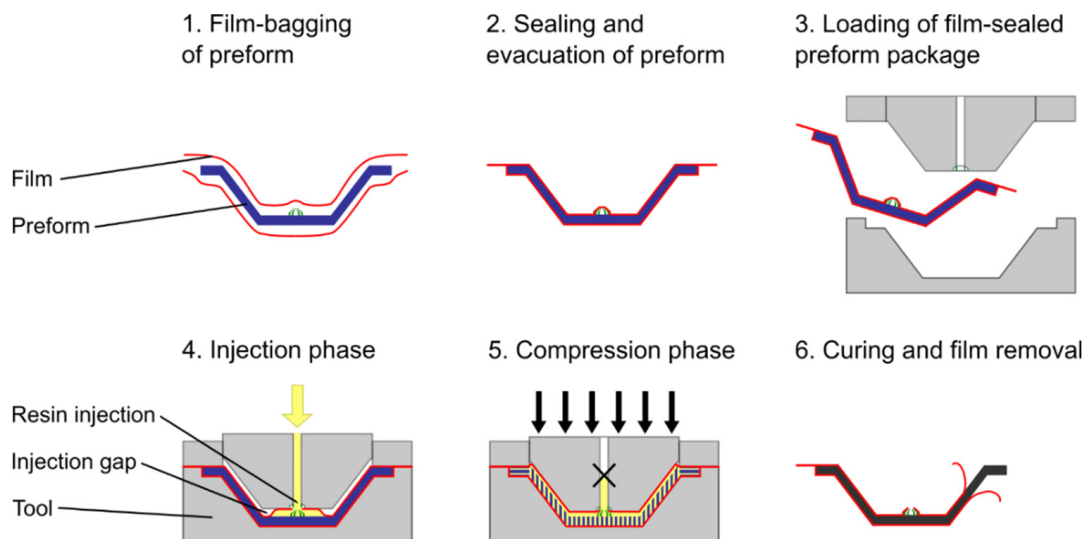


Figure 1. Schematic illustrating the principal steps of the film-sealed compression resin transfer molding process cf. [10].

A frequently reported issue in closed mold liquid composite molding processes is so-called edge race-tracking, which is theoretically preventable, yet with an effort that is usually not practical. Specifically, the preform dimensions need to be negatively tolerated in relation to the cavity in-plane dimensions to enable the preform to be placed inside the cavity and to minimize the risk of fiber pinching, which can be damaging to the tool. Thus, a small channel or area is created between the preform edge and the cavity wall that has low resistance to resin flow. During injection, local inhomogeneous flow front velocities develop inside the cavity that drastically change the preform impregnation pattern. This effect is commonly referred to as edge effect or (edge) race-tracking [12].

Multiple studies investigated the effect of edge race-tracking on the preform impregnation during resin transfer molding (RTM). In contrast to the CRTM process, the preform-containing tool during RTM is completely closed before the resin is injected, leading to a predominant in-plane flow during the preform impregnation. In RTM flow visualization experiments of the edge race-tracking effect, Hammami et al. [13] and Bickerton and Advani [14] showed that the preform impregnation pattern is drastically changed due to an advancing flow inside the edge race-tracking channel and an additional lateral flow from the channel into the preform. Besides changes to the flow pattern, Bickerton and Advani [14] observed in their experiments that the presence of an edge race-tracking channel also reduces the injection pressure at constant flow-rate injection or the filling time of injections at constant pressure. Han and Lee [15] performed experiments in which a flat preform was placed centrally in the cavity surrounded by edge race-tracking channels. Injecting the resin into the preform-free space, the flow advances along the edge race-tracking channels around the preform and eventually fills it transversely from all four sides. Thus, an encapsulated dry preform section is formed in the center of the preform. The flow advances until a pressure equilibrium is reached between the fluid pressure of the impregnated preform sections and the gas pressure in the encapsulated dry preform section. At the point of pressure equalization, the dry preform section cannot be further compressed, commonly referred to as a dry spot or macro void. Parts containing macro voids are typically rejected in industrial FRP production and therefore need to be avoided by appropriate process control strategies.

Different attempts have been presented in the literature to control the preform impregnation and diminish the edge race-tracking effect during RTM processing. These can be divided into passive and active process control strategies. In passive strategies, the objective is to reduce the lateral inwards or outwards flow between the preform edge and a potential race-tracking channel by manipulating one of the three involved factors: preform edge, race-tracking channel or injected resin. A well-established approach is to increase the resistance to resin flow of the preform edge by circumferentially increasing its fiber volume fraction (over-compacting) [16,17]. This can be achieved through design features of the tool such as a reduced cavity height [18] or incorporation of additional material [19–21]. Instead of over-compacting the preform edge to reduce a lateral race-tracking flow, the preform edge can be sealed by applying sealant between individual layers [22] or on top of the preform before the tool is closed [23]. As for the preform edge, the race-tracking channel can be sealed by blocking it with impermeable material prior to the preform injection [24–26], or the flow resistance of the channel can be increased by filling it with low permeable material [21,26,27]. Other passive strategies involve local heating or cooling of the tool cavity to change the resin viscosity and therefore adjust the local flow front velocity inhomogeneity caused by the race-tracking effect [28,29].

In contrast to passive strategies, active process control strategies use sensors to detect the actual flow front progression inside the tool and take corrective action in case a disturbed flow is detected, to prevent the formation of macro voids. Nielsen and Pitchumani [30] presented an active control strategy in which a flow disturbance is tracked in real-time and corresponding data is processed by a controller. The controller employs an artificial neural network, trained by process simulations, to adjust the injection pressure of three inlet ports along the inlet side of the mold. Lee et al. [31] presented an active control

method at which the flow is observed via sensors feeding the information back to a control unit that either adjusts the injection pressure or opens auxiliary gates. The latter attempt to sense the flow front shape and correct a disturbed flow by strategically opening or closing auxiliary gates was also investigated by other researchers and was shown to prevent macro void formation due to flow disturbances such as edge race-tracking [32–36]. Edge race-tracking occurs in industrial FRP production sporadically due to tolerances of preform cutting and placement inside the cavity. The presented active control strategies have the clear advantage that they can sense and adjust the flow in real time but are complex in tool and controller design, adding costs for associated sensors and actuators. In contrast, passive strategies are static means to control the resin flow. Nevertheless, in particular, one passive strategy, the over-compaction or pinch-off of the preform edge, has been proven to be effective and easy to implement, which is why it is a common control strategy for RTM applications [5,37–39].

Despite the extensive investigations on edge race-tracking effects during RTM, a knowledge gap still exists for edge race-tracking effects in the CRTM process and how effects can be controlled during CRTM processing. An initial investigation via numerical CRTM simulations has been presented in [40], but no experimental validation has been conducted yet. Therefore, this paper presents flow visualization experiments of the FS-CRTM process studying the effect of edge race-tracking and investigating a passive process control strategy to diminish edge race-tracking. Figure 2 illustrates the hypothesis of the anticipated flow pattern during the FS-CRTM experiments, considering the numerical results in [40]. Due to spatial constraints of the test rig, preforms with a small geometrical aspect ratio are used in this paper to investigate the FS-CRTM process with injection gap. According to [7,8,40], an in-plane filling of the injection gap is anticipated during the injection phase followed by a through-thickness impregnation of the preform during the compression phase for experiments without a race-tracking channel as illustrated in Figure 2a. By cutting the preform slightly smaller than the in-plane dimensions of the cavity, an edge race-tracking channel is created as shown in Figure 2b. Due to the spatial connection between the injection gap and the race-tracking channel, it is anticipated that besides the injection gap, the channel is also filled during the injection phase. During the compression phase, the preform impregnation pattern is predicted to change to a superimposed flow of through-thickness flow from the injection gap above the preform and a simultaneously occurring in-plane flow from the race-tracking channel [40]. To diminish the flow disturbing effect of edge race-tracking, attractive features of the FS-CRTM process are exploited, i.e., the injection gap is isolated from the edge race-tracking channel and the preform edge is pre-compacted to the final part thickness, as suggested in [10,40]. During the suggested passive flow control strategy, the resin is distributed inside an injection gap that covers only the central section of the preform top surface as shown in Figure 2c. Closing of the central tool segment above the localized injection gap initiates a flow pattern that is intended to impregnate the central preform section under the injection gap predominantly in the through-thickness direction, progressing further through the pre-compacted preform edge predominantly in the in-plane direction. Hence, the goal of the passive flow control strategy is to establish a robust FS-CRTM flow pattern that strategically directs the flow from the preform center towards its edge. A potential edge race-tracking channel is, therefore, filled late in the process and potential flow disturbing effects are diminished [40]. The research findings from this paper elucidate realistic CRTM flow patterns in preforms of small geometrical aspect ratios in which edge race-tracking is difficult to avoid. Further, investigating this passive flow control strategy may enable a more robust CRTM process design by diminishing edge race-tracking effects and lower production cycle times by relaxing requirements on preform cutting and placing tolerances.

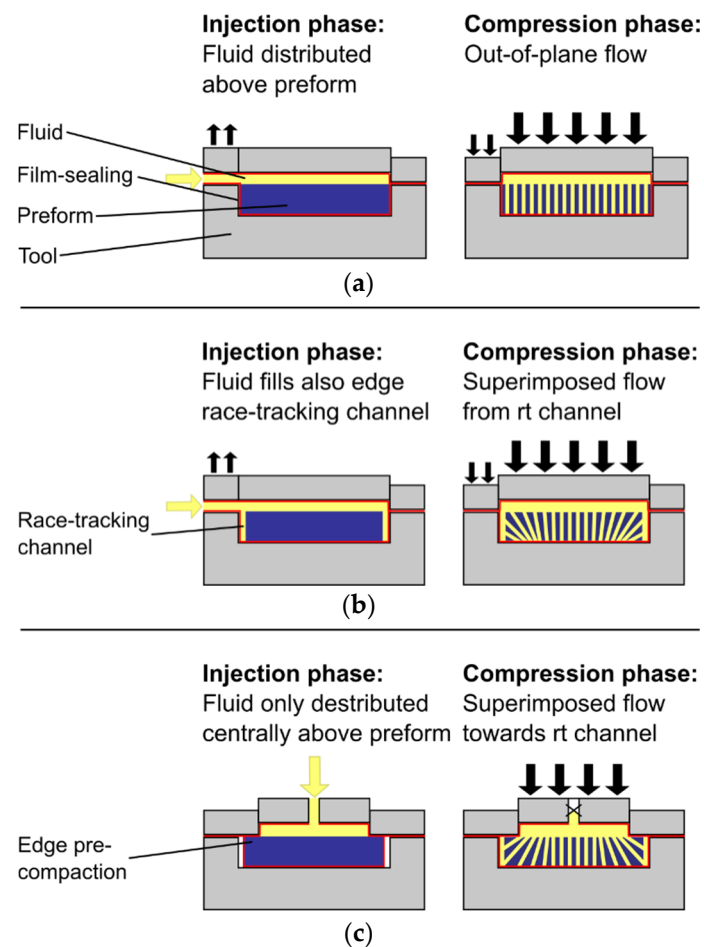


Figure 2. Hypothesized FS-CRTM flow experiment scenarios of preforms of small geometrical aspect ratio: (a) without edge race-tracking (rt) channel; (b) with edge race-tracking channel; (c) applying a passive flow control strategy to diminish the edge race-tracking effect.

2. Experimental Setup, Materials and Methods

2.1. Flow Visualization Setup

A novel test rig was developed to perform the flow visualization experiments for the FS-CRTM process. Figure 3 shows the test rig with its three main components: injection unit, cavity unit, and the control and data acquisition unit. The flow visualization test rig was designed to study the injection and compression phase of the FS-CRTM process on a laboratory scale. A transparent mold design enables the preform impregnation on its top and bottom side to be observed. Sensors recording injection pressure, compression force, and tool gap height history facilitate the comprehensive investigation of the FS-CRTM process. A schematic depicting the test rig with its tubing and wiring is shown in Figure A1 in Appendix A. Additionally, Table A1 in Appendix A lists the manufacturers and types for all purchased components and sensors.

The injection unit is designed to evacuate the preform to a defined pressure level and facilitate the injection of a constant fluid volume at a controlled pressure. Its main actuators are a vacuum pump and a pressure pot with the pneumatic-hydraulic converter (PHC), with the latter being a central component for this experimental setup. A system of tubes and valves ensures the PHC and all tubing between the PHC and the mold are filled with fluid prior to an experiment (see Figure A1). Transparent tubing is used to allow visual control of a bubble-free filling. Tubes and PHC are filled shortly before every experiment with fluid from a temperature-controlled reservoir to ensure comparable fluid viscosities between the experiments. The PHC is equipped with an adjustable limit stop to manually set the volume of injected fluid with high reproducibility. The injection process

is controlled and automated via a LabVIEW program (National Instruments Corp., Austin, TX, USA) that regulates the pressure applied to the PHC and opens and closes the inlet slider of the cavity.

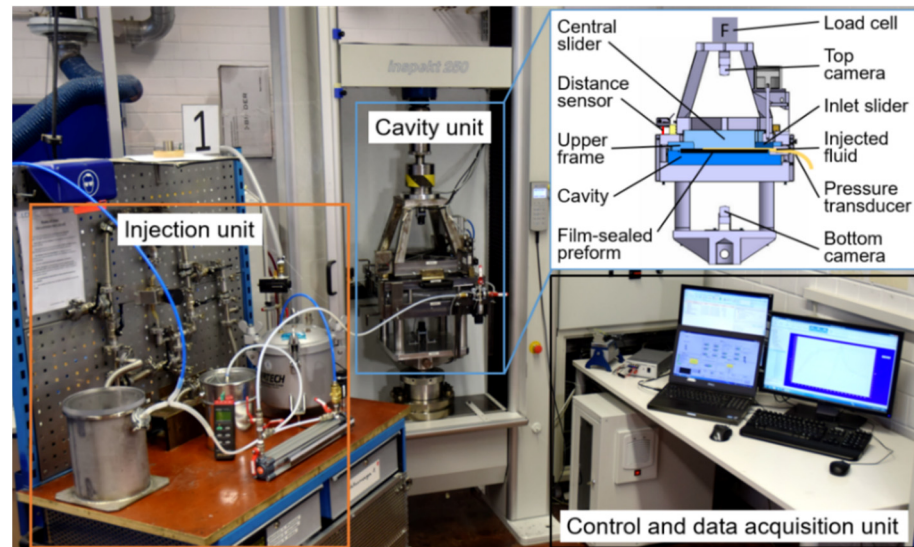


Figure 3. Flow visualization test rig grouped in its three main units. Inset on top right illustrates the cavity unit with labeling of its main components and sensors.

The preform impregnation takes place inside the cavity unit, which contains all of the main sensors to monitor the flow visualization experiment. The film-sealed preform package is placed in the transparent cavity and connected to the inlet and vent hoses of the injection unit. The cavity is designed to accommodate planar preforms of different in-plane and thickness dimensions by using different inlay spacers. The transparent upper tool, made of polymethylmethacrylate (PMMA), is composed of three components as seen in the sectional drawing in Figure 3. It consists of a circumferential upper frame that compresses the outer film layers and pre-compacts the preform edge depending on the preform size. Inside the upper frame, the central slider can be moved vertically to realize the active tool movement during the FS-CRTM process. The injection of the fluid is realized via a lateral inlet, which is opened by the inlet slider, which is a movable 40 mm wide section of the upper frame. The cavity, upper frame, and central slider are stiffened by steel structures to minimize their deformation, thus resulting in local fiber volume changes inside of the transparent tool. The stiffening structure of the lower cavity is affixed to the lower, static portion of the universal testing machine (UTM), see Figure 3. The upper frame and cavity are bolted together via their stiffening structures, and the inlet slider and its pneumatic actuator are attached to the stiffening structure of the upper frame. The central slider and its stiffening structure are connected to the movable crosshead of the UTM. Two cameras are mounted inside the stiffening structures of the central slider and lower cavity to monitor the preform impregnation. The injection pressure is logged via a pressure transducer in the feeding line of the inlet. The force applied to the central slider is recorded via the load cell of the UTM to enable the force history during the compression phase of the process to be recorded. Two laser triangulation sensors (LTS) record the gap height by measuring the distance between the stiffening structures of the movable central slider and the static upper frame.

The control and data acquisition unit is split in two parts, separately controlling the injection and compression phase of the FS-CRTM process. A detailed process control sequence is established and semi-automated via a LabVIEW program in which fluid injection is initiated by the operator and afterwards performed autonomously. Visible and acoustic signals at the end of the injection phase indicate to the operator to start the automated closure sequence of the central slider via the control software of the UTM, LabMaster (Hegewald & Peschke, Nossen, Germany). The established process control sequence enables a reproducible FS-CRTM process in which the idle time between the two manually initiated phases is reduced to only a fraction of the process time, specifically 0.5 ± 0.2 s (average \pm standard deviation) for all experiments in this paper. Data acquisition from all main sensors is implemented into the LabVIEW program except for the force recording, which is recorded via LabMaster.

2.2. Materials

A common reinforcement structure for automotive applications is built of non-crimp fabric (NCF) containing carbon fibers [4,41–43]. Thus, the stitched, biaxial NCF material SIGRATEX[®] C B310-45/ST-E214/5 g manufactured by the SGL Group (Wiesbaden, Germany) was chosen for this study, containing the carbon fiber SIGRAFIL[®] C T50-4.4/255-E100 [44]. The NCF material has a nominal specific mass of 318 g/m^2 including a pre-applied powder binder of 5 g/m^2 on one side of the fabric. Two different batches of the SIGRATEX[®] NCF material formed the preforms used in two separate studies for this paper. Due to manufacturing tolerances, the specific mass of the NCF batch used for studying edge race-tracking was measured to be $320 \pm 1 \text{ g/m}^2$, and the batch used for studying the passive flow control strategy was $316 \pm 1 \text{ g/m}^2$ (average \pm standard deviation).

The preforms consisting of the NCF material were encapsulated in thermoplastic films. A cost-effective multilayer polyamide/polypropylene (PA/PP) film was developed for FS-CRTM production due to its favorable mechanical properties at process temperatures of $80\text{--}120$ °C, chemical resistance to thermoset resin systems, low gas permeability of air, and good weldability [45]. However, in the present investigation, flow visualization experiments were performed at room temperature to study the preform impregnation in the FS-CRTM process. Therefore, a thermomechanical characterization was performed to substitute the PA/PP film at process temperature with a film of comparable mechanical properties at room temperature. A polyethylene low-density (PE-LD) film manufactured by Sokufol (Limburg, Germany) was identified to be a suitable replacement. The film is 0.1 mm thick and optically transparent to enable an observation of the FS-CRTM preform impregnation.

The presented study focuses only on the mold filling of the FS-CRTM process. Thus, a reactive thermoset resin was substituted with a non-reactive fluid of comparable flow characteristics to ease the experimental procedure. Sunflower oil was chosen due to its comparable flow characteristics and its Newtonian behavior. Its viscosity was measured with a cone-plate measuring system on a Modular Compact Rheometer (MCR) 302 (Anton Paar, Graz, Austria) at a shear rate of 100 s^{-1} to be approximately $54 \text{ mPa}\cdot\text{s}$ at 25.5 °C.

2.3. Preform Preparation and Film-Sealing

Structural FRP parts for automotive applications are commonly designed to contain a fiber volume fraction (FVF) of $50\text{--}60\%$ [5,46]. Therefore, the preforms for the presented studies were composed of 15 layers of the SIGRATEX[®] NCF material [44] aiming at a FVF at the upper boundary of approximately 60% . The individual layers were cut to an oversized dimension of 30.2 mm larger than the final preform in-plane size of 209.8×209.8 mm for the edge race-tracking experiments and 227.8×227.8 mm for the flow control study experiments without a race-tracking channel. A symmetric lay-up was created by flipping and rotating the lower seven layers by 90° . The binder was activated at $170 \text{ }^\circ\text{C} \pm 10$ °C via infrared heating and debulked under vacuum pressure. To ensure a good quality cut of the preform edges, cutting of the individual layers as well as of the activated preform to its final

dimensions was done using a CNC cutting table (M-1200 CV, Zünd, Altstätten, Germany). While it was observed that the cutting dimensions of individual NCF layers agreed well with the nominal dimensions, the cutting dimensions of thick preform stacks deviated by approximately 1 mm and 0.5 mm from the nominal dimensions depending on the principal axis. Due to the deviation of cutting dimensions, a constant target race-tracking channel of 2 mm and 4 mm could not be realized as initially anticipated for the race-tracking study. Correcting steps were implemented during the cutting of the preforms for the flow control study, which is why a more homogeneous theoretical channel width was realized for this test series. The exact dimensions and corresponding theoretical channel widths of all preforms are listed in Table A2 in Appendix A.

Preliminary tests exhibited severe fiber washout at the inlet section of the tested preform. The upper layers of the preform were pushed back or even flipped, which may lead to a disturbed fluid flow and increased compression forces due to a locally increased FVF. The cause of the fiber washout was traced back to the lateral inlet design. The fluid is guided inside the film-sealed preform package over the edge section of the lower cavity hitting the protruding layers of the uncompressed preform. To prevent fiber washout, a fluid transition zone of 60 mm width was implemented as illustrated in Figure 4. Adhesive tape [47] was applied connecting the inner side of the lower film to the top surface of the preform guiding the fluid flow and preventing preform washout at the inlet section. For preforms of the race-tracking study, the overlap was determined to be 4 mm wide to balance a minimal disturbance of the through-thickness preform impregnation and sufficient tape adherence to prevent tape separation during preform and test preparation. For preforms of the flow control study, the tape overlap of the transition zone was increased to 9 mm, representing the width of the pre-compacted preform edge. The impermeable character of the tape was intentionally used during the flow control study to avoid an impregnation of the preform edge during the injection and therefore simulate a direct injection into the isolated central injection gap. Due to the design of the test rig, the fluid can only be injected laterally, whereas, and hence, the intended central injection, as indicated in Figure 2c, is simulated via a direct, lateral injection into the central injection gap realized by the fluid transition zone and the applied impermeable tape in the section of the pre-compacted preform edge. The concept of a fluid transition zone was adapted to the experiments with a race-tracking channel by cutting the preforms to butt joint the cavity wall at the inlet over a width of 60 mm, neighboring the circumferential race-tracking channel as illustrated in Figure 4.

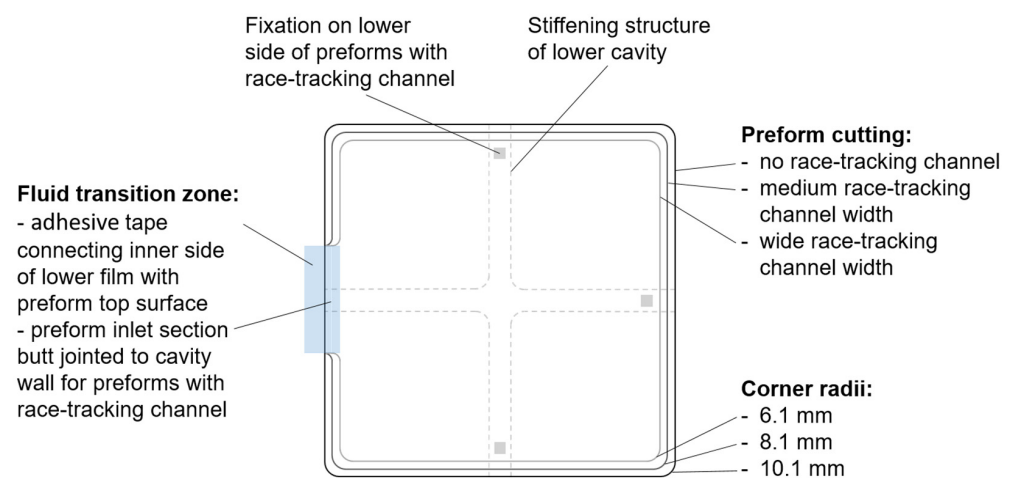


Figure 4. Schematic illustration of preform shapes including fluid transition zone and preform fixation on lower side of preforms with a race-tracking channel.

The film-sealing of the preform is a critical step in the FS-CRTM process chain. While the film-sealed preform package needs to be air- and liquid-tight, it also needs to be free of wrinkles. In the preform section, wrinkles of the film could cause imprints on the part surface or result in out-of-plane wrinkles of the fiber structure. In the outer tool section, wrinkles of the two touching films could result in overlapped material that is thinned or even torn during closure of the upper frame. Thus, the film-sealed preform package could leak, bearing a high risk of an unsuccessful preform impregnation. To minimize film wrinkling and to ensure a repeatable process, a film-sealing station was developed as shown in Figure 5. At the beginning of the film-sealing process, a lower film sheet of 670×420 mm was spanned on the deep drawing post. The film was then manually heated via a hot air gun while vacuum was applied below the film, deep drawing it into a negative form in the shape of the cavity of the flow visualization test rig. The preform was then placed on top of the lower film inside the cavity. The exact central positioning of the preforms for experiments with race-tracking channels was realized via 3D-printed spacer blocks placed between preform edge and deep drawn film at the cavity wall. Small 5×5 mm squares of double backed tape [48] were applied near the preform edges as illustrated in Figure 4 to affix the preform in its central position as well as to prevent any lift-off and flushing of the preform. To minimize a disturbed observation of the preform impregnation, the fixation points were placed above the stiffening structure of the lower cavity section not visible in the later post-processing of the flow visualization experiments. After covering the lower film and positioned preform with an upper film sheet, the two films were sealed on all four sides via impulse welding. The film-sealing station was designed to adjust and control the pressure and heat application during the welding process. Teflon films were placed between the thermoplastic films at the locations where the inlet and vent hose are later bonded via sealant tape [49]. An inlet passage was created to prevent lateral outflow of the fluid inside the film-sealed preform package between inlet hose location and injection gap. The inlet passage was realized by manually welding the films on both sides of the inlet and sealing the section on top of the fluid transition zone with sealant tape. To ensure a complete evacuation of the preform, a cord was threaded through the vent hose and fixed on the lower film connecting the vent with the preform. All features and components of the film-sealed preform package are shown in Figure A2 in Appendix A.

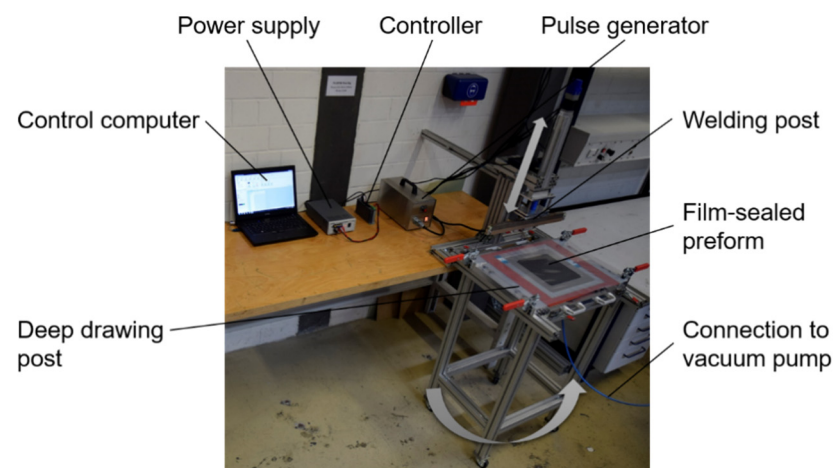


Figure 5. Components of the film-sealing station for preforms.

2.4. Experimental Procedure

The experimental procedure of the flow visualization experiments was divided into three phases: preparatory work, experiment execution, and data post-processing. At the beginning of the preparatory work, the limit stop of the PHC was adjusted to the predefined fluid volume of the test series. The correct setting was checked by filling and

metering the PHC five times prior to each test series. Afterwards, the limit stop setting was kept constant throughout the test series to ensure a reproducible injected fluid volume for each experiment. In the next step, the film-sealed preform package was evacuated to the desired vent pressure of the experiment and its thickness was measured. By knowing the thickness of the film-sealed preform package, the gap height of the central slider was calculated and entered into the control sequence for the central slider movement in the LabMaster software. Adjusting the gap height for each experiment of the test series ensured a constant injection gap between preform top side and the central slider. The injection pressure was adapted by defining the pressure inside the pressure pot via the LabVIEW program. The pressure pot level was set to an increased value to compensate for pressure losses inside the tubes and the PHC. Furthermore, the cavity was adjusted to fit to the preform dimensions of the test series. First, the cavity height was adjusted by placing a transparent inlay plate. A thin layer of glycerin was applied between cavity bottom wall and inlay plate to improve the image quality for the lower camera. Second, inlay frames were inserted to adapt the cavity to the in-plane dimensions of the preform. Once the cavity was prepared, the film-sealed preform package was connected to the tubes of the injection unit, evacuated to the desired vent pressure of the experiment, and placed inside the cavity. Special care was taken to precisely place the preforms for experiments with a race-tracking channel. First, the transition zone at the inlet section of the preform was butt joined to the inlay frame defining the race-tracking channel at the inlet and vent side. Second, an equal lateral race-tracking channel space was adjusted with the aid of 3D-printed spacers. The latter were removed after the preform was positioned. Then, the upper frame was placed by positioning it relative to both sliders to ensure smooth sliding during their vertical movements. The lighting conditions were checked and adjusted before each experiment to ensure a consistent high-quality process observation on the top and bottom side of the preform. Finally, the PHC and all tubes between the PHC and the inlet slider were evacuated and filled with fluid. In contrast to the fluid reservoir, the PHC and tubes were not temperature controlled, which was why this step was executed last in the preparatory work to minimize the time the fluid was exposed to a potential difference between defined fluid temperature and ambient temperature.

The actual flow visualization experiment was executed by launching the LabVIEW program, recording all sensor and camera data. Subsequently, the LabMaster program was started, which performed the lowering of the central slider to the gap height for the experiment. After double-checking the correctness of all set process parameters and the recording of all relevant data, the operator started the fluid injection in LabVIEW. At the end of the injection, optical and acoustic signals indicated to the operator to initiate the closing sequence using the LabMaster program, moving the central slider at a constant closing speed until a pre-defined final closing position was reached. The closing sequence was held in the final closing position until the operator actively terminated the experiment after complete filling of the preform or a defined time.

The final phase, data post-processing, involved the following tasks. A data post-processing script was programmed using the software MATLAB® (MathWorks, Natick, MA, USA). In a first step, the raw data files recorded by the LabVIEW and LabMaster programs were merged into a single dataset. The latter was combined with important process characteristics and calculated response data into a single output file. In a second step, images captured by the cameras during testing were post-processed to identify the flow front progression during the different phases of the FS-CRTM process and to calculate the area filling ratio (AFR) history for the race-tracking channel as well as for the top and bottom side of the preform. The AFR represents the filling of the preform surface excluding: (i) the preform section that is hidden by the stiffening structures and (ii) the fluid transition zone of experiments with race-tracking channels. Due to limitations of the used post-processing algorithm, flow front features involving sharp corners (i.e., a non-differentiable point on a curve) cannot be detected. The diagonal stiffening structure on the preform top side introduces such features, and hence, complete filling of the preform

top side is defined as a maximum AFR of approximately 97%. Calculating the AFR of the race-tracking channel proved to be challenging using the chosen methodology. While 80–90% of the channel area could be analyzed for experiments with medium race-tracking channel width, only a channel area approaching 50% could be assessed for experiments with the wide channel width. Reasons for these challenges were optical artifacts caused by the reflective and translucent nature of the test fixture and disturbed lighting when the glycerin film below the PMMA inlay was disturbed. These issues can lead to AFR values below 100% and temporal reductions in the AFR progression for the race-tracking channel, which is physically incorrect. Consequently, any AFR data for the race-tracking channel must be interpreted with caution. Even so, qualitative information about the point in time at which the race-tracking channel was filled was verified manually and was therefore included in the presented analysis.

2.5. Experimental Plan

Two flow visualization test series are reported in this paper. First, the effect of edge race-tracking on the preform impregnation of the FS-CRTM process was investigated. Second, a passive flow control strategy to diminish the race-tracking effect during FS-CRTM preform impregnation was studied. The first test series is herein referred to as ‘race-tracking study’ or ‘RT study’, while the latter as ‘flow control study’ or ‘FC study’. Both studies were performed using the same previously described flow visualization test rig with related boundary conditions. The in-plane dimensions of the central slider are fixed at 210×210 mm with corner radii of 10 mm, while the cavity size below the central slider is adjustable. Since experiments for the RT study require an injection gap spanning over the entire cavity area, the cavity size was set to fit the in-plane dimensions of the central slider. Conversely, the FC study utilized a central injection gap in combination with a pre-compaction of the preform edge to the final part thickness. Therefore, the cavity size was increased for the FC study to in-plane dimensions of 228×228 mm with corner radii of 10 mm. The enlarged cavity was then covered by a split upper tool. While the peripheral section of the cavity was covered by the static upper frame realizing the pre-compaction of the preform edge, the central part was covered by the movable central slider enabling a central, localized injection gap.

The preform in-plane dimensions were adjusted to fit the two different cavity sizes for the two test series. To study the natural preform impregnation pattern for each test design, reference experiments without a race-tracking channel were conducted in triplicate. Preliminary tests revealed that preforms cut to the nominal dimensions exhibited signs of edge race-tracking. To suppress randomly occurring edge race-tracking, the preforms of the reference configuration were cut slightly larger than the nominal dimensions as suggested in [50]. Further, two configurations of preforms with medium and wide race-tracking channels were cut for each test series as previously explained and illustrated in Figure 4. Akin to the reference configuration, each experimental scenario with a race-tracking channel was conducted in triplicate. The exact preform dimensions and their theoretical race-tracking channel widths, neglecting placement tolerances, are listed in Table A2 in Appendix A.

In contrast to the varied preform dimensions, the process conditions were kept constant or were adapted to the changed cavity sizes of the two test studies. As listed in Table 1, the pressure pot was set to a target differential pressure of 370 kPa relative to ambient pressure. This setting was chosen to compensate for flow friction losses aiming at a differential stagnation pressure of 300 kPa at the inlet prior to fluid injection. Before each experiment, the target differential vent pressure was manually adjusted to -90 kPa relative to ambient pressure. The injected fluid volume was calculated based on the targeted fiber volume fraction of 60% and the cavity volume of the corresponding study at a target cavity height of 4.6 mm. The reported injected fluid volumes in Table 1 are the average and standard deviation of five metered and measured injections prior to each test series. To achieve complete filling of the injection gap during the injection and a subsequent through-

thickness flow during the compression phase, the volume of the injection gap was set to 66% of the injected fluid volume. The corresponding target injection gap heights are listed for both studies in Table 1. The closing of the central slider was velocity controlled at a target closing speed of 10 mm/min. Preliminary tests revealed some deflections of the test rig. To compensate for this deflection, the target final closing position in the UTM control software was set -0.15 mm below the theoretical position of complete cavity closure for all experiments.

Table 1. Process conditions of experiments for the race-tracking (RT) and flow control (FC) studies.

Target Pot Pressure ¹	Target Vent Pressure ¹	Injected Fluid Volume		Target Injection Gap Height		Target Closing Speed	Target Final Closing Position
[kPa]	[kPa]	RT study	FC study	RT study	FC study	[mm/min]	[mm]
370	-90	93.6 ± 0.5	102.2 ± 0.4	1.42	1.55	10	-0.15

¹ Differential value relative to ambient pressure.

3. Results and Discussion

The present section reports the findings from the test series conducted for the RT study and the FC study. The target process conditions, as presented in the previous section, were monitored and were found to be well within limits, as listed in Table A3 in Appendix A. In the following, test data are presented in a sequence of graphs that are similar for both test series. First, the evolution of important process variables over time are depicted (see, e.g., Figure 6). Here, data for the gap height of the central slider, which was computed as the average of data from two laser triangulation sensors (LTS), are depicted in blue. The force acting on the central slider is shown by an orange curve, recorded via the load cell of the UTM. To draw conclusions on the preform impregnation, AFR histories of the preform top and bottom side as well as of the race-tracking channel, evaluated via post-processing of recorded images, are plotted as black curves. In addition to quantitative process information, qualitative information in the form of flow front progression visualizations for the preform top and bottom side is also presented (see, e.g., Figure 7). The experiments involve three phases. The injection phase takes place between the process start at 0 s and the 'injection end'. The compression phase follows the injection phase and finishes at the 'compression end', which is simultaneous with the beginning of the holding phase. The three phases are distinguished by marked end times in the quantitative overview plots and are labeled in the legend of the qualitative flow front progression plots. Note that only one representative experiment for each configuration is presented in this section; remaining experiments are included in Appendix A of this paper.

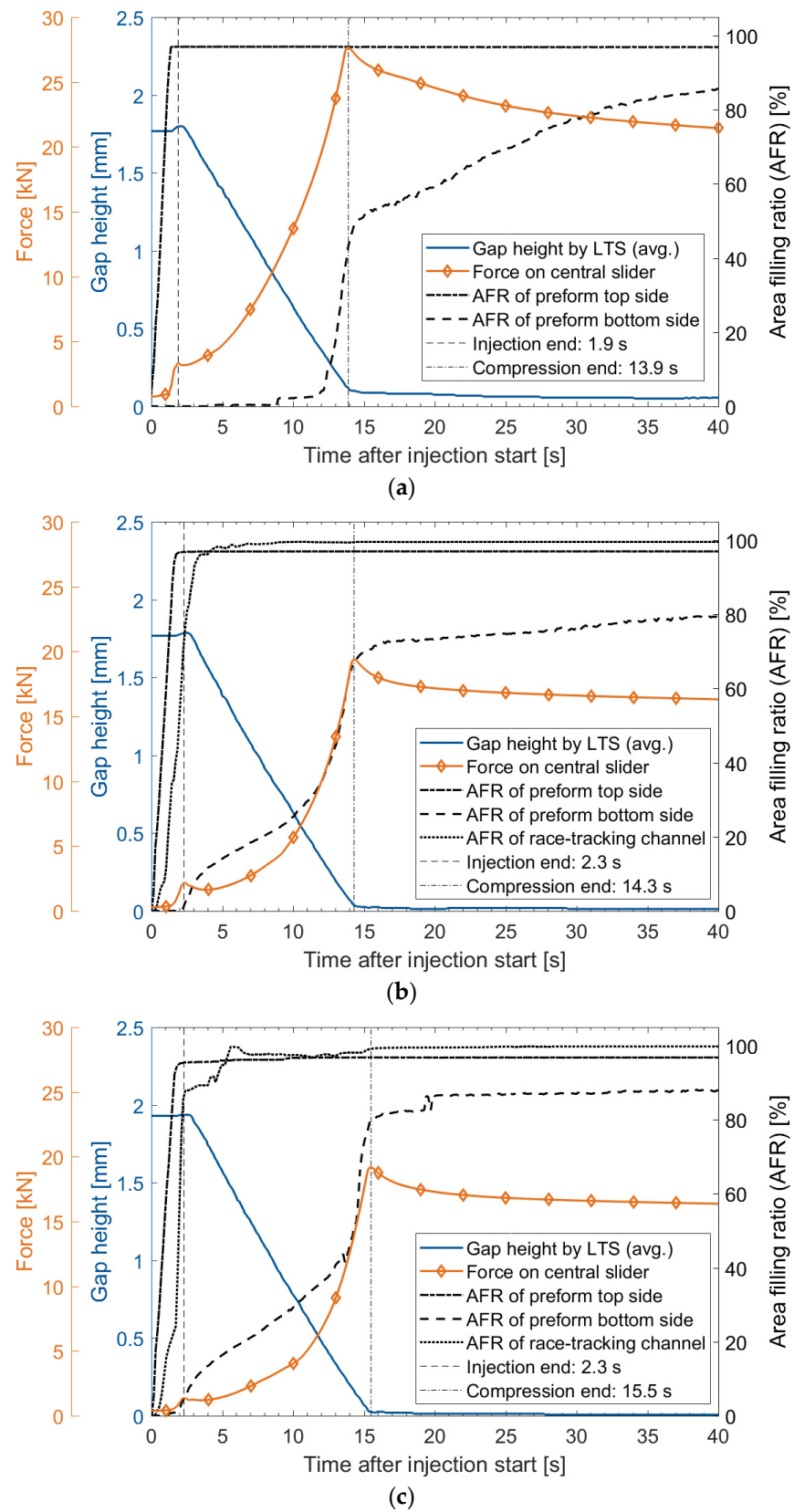


Figure 6. Overview of important process variables during FS-CRTM experiments of the race-tracking study: (a) no race-tracking channel—vc-#3; (b) medium race-tracking channel width—mrt-#3; (c) wide race-tracking channel width—wrt-#1 (LTS = laser triangulation sensor).

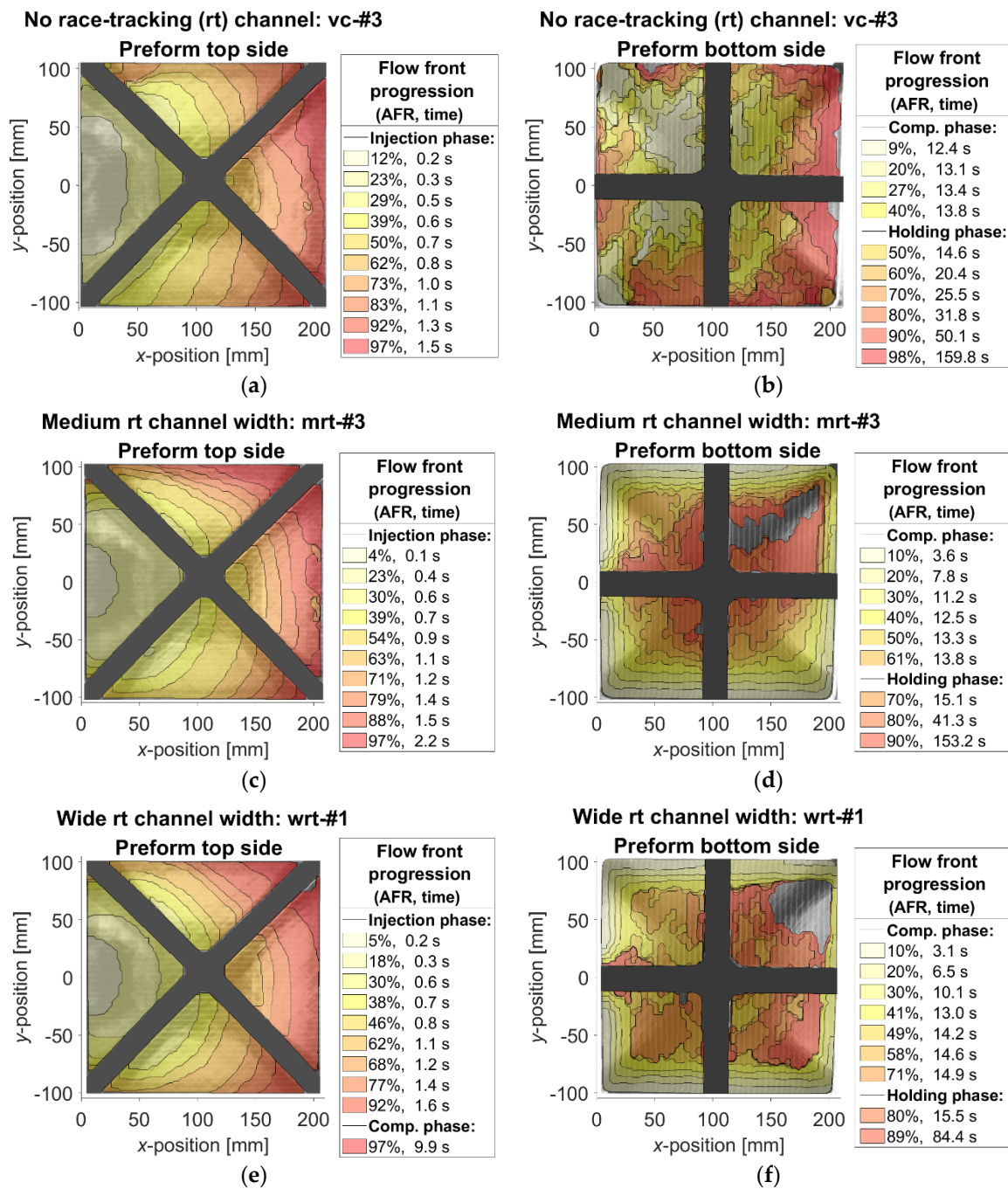


Figure 7. Flow front progression of FS-CRTM experiments of the race-tracking study: (a,b) no race-tracking (rt) channel—vc-#3; (c,d) medium race-tracking channel width—mrt-#3; (e,f) wide race-tracking channel width—wrt-#1 (AFR = area filling ratio).

3.1. Race-Tracking Study

The race-tracking (RT) study investigates the edge race-tracking effect by quantitatively (Figure 6) and qualitatively (Figure 7) comparing FS-CRTM flow visualization experiments without a race-tracking channel (scenario (a), indicated by an identifier with the test number, e.g., ‘vc-#1’ for the first test) with experiments with a medium (scenario (b), ‘mrt-#1’) and a wide race-tracking channel (scenario (c), ‘wrt-#1’). Comparing the injection phase of all three experimental scenarios in Figure 6, the presence of a race-tracking channel is not seen to noticeably change the end time of the injection. Furthermore, it is observed that the AFR of the preform top sides of all three experimental scenarios increases linearly, with complete filling indicated before the end of the injection phase, which was the intent

of the designed process. Recalling that the gap height was set to create an injection gap volume of 66% of the injected oil volume, the injection gap volume was therefore filled before the complete oil volume was injected, which was intended to produce a predominantly out-of-plane preform impregnation during the following process phases.

Towards the end of the injection phase, the force rises for all scenarios in Figure 6. Simultaneously, the gap height increases slightly even though the UTM position control was programmed to hold the central slider in a constant position until the end of the injection phase. Both observations indicate an increase in cavity pressure between the complete filling of the preform top side and the end of the injection, resulting in an increased reaction force acting on the central slider and an associated deformation of the test rig. These effects are reduced with increased race-tracking channel width in scenarios (b) and (c) in Figure 6. As for the effects themselves, their reduction is also traced back to the process design, which keeps the cavity size constant and reduces the preform size to realize experiments with edge race-tracking. The injection gap, spanning over the complete cavity size, is spatially connected to the race-tracking channels. At the presence and increase of a race-tracking channel, the preform-free space inside the cavity is increased, which provides more space to distribute the injected oil volume, reducing the cavity pressure increase after full filling of the injection gap and race-tracking channel.

The spatial connection between the injection gap and race-tracking channel also causes an early filling of the race-tracking channel as seen in scenarios (b) and (c) in Figure 6. The AFR of the race-tracking channels rises shortly after the injection start, increasing quickly, with the channel largely being filled at the end of the injection phase. The short time delay observed before the rise of the channel's AFR after the injection start is caused by the preform design, which incorporates the fluid transition zone to guide the fluid from the lateral inlet onto the preform, as illustrated in Figure 4.

The flow front progression plots of Figure 7 show a similar filling pattern on the preform top side for all three experimental scenarios. Due to the injection of fluid into the injection gap above the preform, the shown flow front progression on top of the preform is correlated to the filling of the injection gap itself. Thus, the injection gap was filled from the inlet slider ($x = 0$, $-20 \text{ mm} < y < 20 \text{ mm}$), radially progressing towards the vent side ($x > 200 \text{ mm}$). A homogeneous, repeatable flow pattern was observed for all experiments with a race-tracking channel, while the flow front progressions of experiments without a race-tracking channel were slightly disturbed, which is explained as follows. To prevent edge race-tracking in experiments without a channel, the preforms were intentionally cut slightly larger than the cavity size. Cutting tolerances, which differed in the two principal directions of the CNC cutting table, resulted in out-of-plane wrinkles over the width of the preform after placing them in the cavity. The flow pattern in the associated experiments was slightly affected by the out-of-plane wrinkles as seen in Figures 7a and A5a,c in Appendix A. Moreover, the image post-processing script misinterpreted sections of large wrinkles at, e.g., $x = 180 \text{ mm}$ of Figure A5a,c in Appendix A to be filled too early which thus need to be neglected during a general interpretation of the flow front progressions. Therefore, excluding these ambiguous sections of the flow front progression, a similar flow pattern inside the injection gap, from the inlet slider radially towards the vent side, was observed for all three experimental scenarios.

After the injection ended, the compression phase was initiated, which is indicated in Figure 6 by a decreasing gap height. Even though the UTM position was lowered to -0.15 mm as the final tool closing position to compensate for tool deformation, the measured gap height in scenario (a) is not completely closed at the end of the compression phase. The incomplete gap closure in combination with the lowered final tool closing position indicates a test rig deformation opposite to the closing direction. Due to this deformation, the closing speed was also slightly reduced from its targeted value of 10 mm/min , evidenced by a departure of the gap height curve from perfectly linear during the compression phase. The non-linearity of the gap height curve towards the end of the compression phase correlates with a strong force increase, depicted in Figure 6a. The

recorded force acting on the central slider increased non-linearly with decreasing gap height and peaks at the end of the compression phase. Applying Terzaghi's law [51] to the FS-CRTM preform impregnation, the recorded force is composed of two components. On the one hand, the fiber structure, i.e., the preform, is compacted to its final thickness, and, on the other hand, the fluid pressure is increased due to the occurring preform impregnation.

While the exact preform impregnation and its out-of-plane flow through the thickness of the preform cannot be observed by the current test method, the arrival of fluid at the preform bottom side can be recorded as indicated by its AFR shown as a dashed black line in Figure 6a. Besides marginal race-tracking in the preform corners, a sudden and steep increase of the AFR of the preform bottom side was recorded towards the end of the compression phase. This near-linear increase in Figure 6a between 12–14 s is visualized in the flow front progression plot of Figure 7b as a patchy arrival of fluid on the preform bottom side. It was observed that the fluid penetrates the preform during the time of the near-linear AFR increase first at the sewing yarns in some areas of the preform, followed by the penetration of the adjacent fiber structure. At the end of the compression phase in Figure 6a, the AFR curve on the preform bottom side changes its shape and progresses with a reduced slope towards full filling during the holding phase of the process. Simultaneously, the force curve relaxes during the holding phase, indicating a viscoelastic behavior of the FS-CRTM preform impregnation. Referring to the gap height after the incomplete gap closure at the end of the compression phase in Figure 6a, it can be observed that the height further reduces during the holding phase and eventually stagnates at the complete gap closure. The observed elastic deformation of the test rig during the holding phase correlates to the viscoelastic behavior of the FS-CRTM preform impregnation. Therefore, it is presumed that the incomplete gap closure causes the incomplete filling of the preform bottom side at the end of the compression phase in Figure 6a. This presumption is supported by the relaxation of the elastic test rig deformation during the holding phase and the simultaneous increase of the AFR of the preform bottom side.

In contrast to the AFR of the preform top side, which is nearly unchanged by the presence of a race-tracking channel, the AFR of the preform bottom side provides insight into the effect that edge race-tracking has on the preform impregnation during FS-CRTM. Comparing the AFR progression of the preform bottom side of the experiment without a race-tracking channel in Figure 6a with the experiments of medium (b) and wide race-tracking channel width (c), an earlier rise of the AFR curve in Figure 6b,c can be observed at the injection end, followed by stagnation during the holding phase. To facilitate a more in-depth analysis, AFR data for the preform bottom side for all experiments are plotted in Figure 8 up to a process time of 160 s. The process end time at 160 s was experimentally determined as the gel point at 100 °C of the snap-cure resin system Araldite® LY 3585/Aradur® 3475 (Huntsman, Salt Lake City, UT, USA) used for composite manufacturing in the automotive industry. Figure 8a shows that the AFR of the preform bottom side for experiments without a race-tracking channel remains approximately zero until a sudden increase at around 12–13 s. In contrast, an early rise in the AFR of the preform bottom side (at approximately 2 s) can be observed for all experiments with a race-tracking channel. Considering the flow front progression of the preform bottom side shown in Figure 7d,f, the observed early increase in AFR can be correlated to the recorded lateral flow from the race-tracking channels toward the preform center.

Two inhomogeneities of the lateral race-tracking flow are observed in Figure 7d,f at the inlet section ($x = 0$, $-20 \text{ mm} < y < 20 \text{ mm}$) and at the vent side ($x > 200 \text{ mm}$). The first inhomogeneity can be explained by the design of the fluid transition zone, which is butt jointed to the cavity wall to guide the fluid onto the preform and prevent fiber washout as illustrated in Figure 4. Thus, there is no race-tracking channel present at the inlet section of the preform, causing the observed inhomogeneity of the lateral flow. The second inhomogeneity at the vent side of the preform is explained by the lateral inlet design and the different theoretical race-tracking channel widths. As illustrated in Figure 7c,e, the fluid filled the injection gap radially from the inlet slider towards the vent side of the

preform where it finally reached the race-tracking channel located there. Additionally, this portion of the race-tracking channel was the narrowest of all four preform sides due to inaccurate cutting dimensions as listed in Table A2 in Appendix A. The combination of both effects caused a delay in lateral preform filling from the race-tracking channel at the vent side ($x > 200$ mm) as observed for all race-tracking experiments of the RT study.

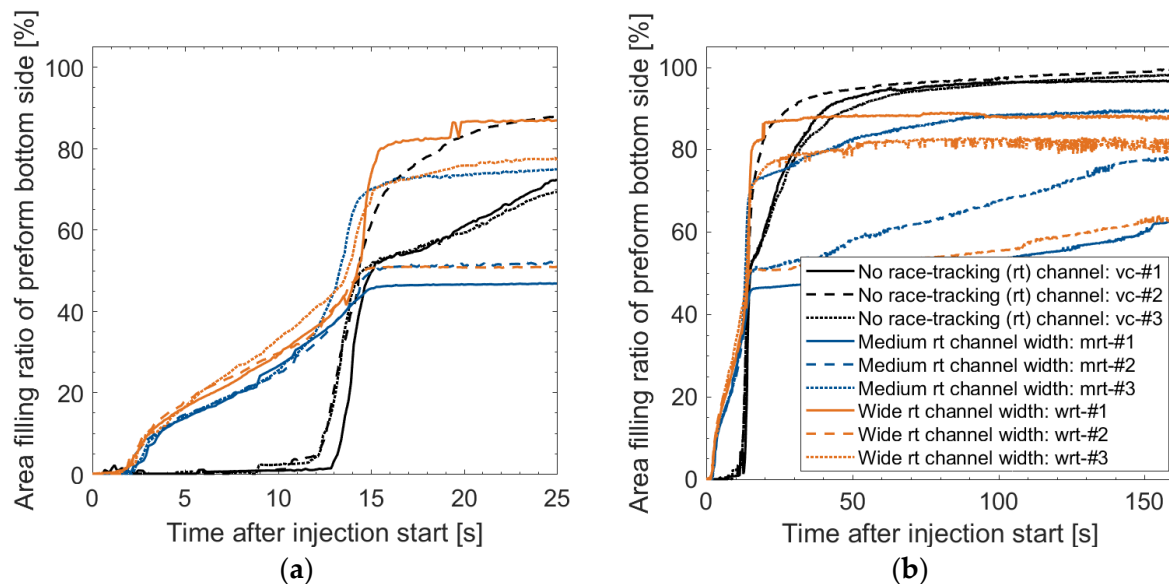


Figure 8. Area filling ratio of preform bottom side: (a) during the first 25 s of the process; (b) until gel time of representative snap-cure resin system. For legend of both plots see (b).

Following the lateral flow and its early AFR rise of the preform bottom side between 3–11 s depicted in Figure 8a, the various experiments with a race-tracking channel exhibit different progressions at the end of the compression phase. While one experiment with a medium and one with a wide race-tracking channel width immediately stagnate, the others increased further with a steeper slope comparable to the initial near-linear AFR increase of the experiments without a race-tracking channel. Looking at the flow front progression in Figure 7d,f as well as in Figure A6b,e in Appendix A, the further AFR increase can be traced back to the arrival of an out-of-plane flow in the center of the preform. The fact that some experiments with a race-tracking channel experience an arrival of the central out-of-plane flow on the preform bottom side and others do not led to a strong deviation of the recorded AFR at the end of the compression phase. While the AFR data for the preform bottom side in experiments without a race-tracking channel further increase during the holding phase towards 100%, the experiments with race-tracking show only a minor increase or complete stagnation of the AFR curves and stay below complete filling of the preform bottom side at 160 s after the process start, as seen in Figure 8b.

The incomplete filling in the experiments with a race-tracking channel resulted in the formation of a macro void. As seen in Figure 7d,f, Figures A5f and A6b,d,e in Appendix A, the macro void is always located on the preform bottom side in its central section, surrounded by the lateral race-tracking flow and, in some experiments, additionally by the out-of-plane flow. The void was caused by two effects: (i) the defined volume of fluid that was injected into the cavity and (ii) the increase of overall porosity inside the cavity when a race-tracking channel is present. With respect to (i), the injected fluid volume, kept constant for the experiments, was determined by the fiber volume fraction of a preform without a race-tracking channel, i.e., the preform fills the complete cavity. For (ii), if the preform is cut significantly smaller than the cavity dimension, to realize a race-tracking channel, then the overall porosity of the cavity is increased, thus providing additional volume to be filled by the fluid. If the fluid volume is not adjusted to the increased porosity

and the race-tracking channel is filled early in the process, then the injected amount of fluid is insufficient to completely impregnate the preform, resulting in the observed macro void.

The size of the macro voids at the end of the process varies largely between the various experiments with medium and wide race-tracking channels as seen in Figure 8b. The strongly varying results prevent any correlation between the macro void size and the race-tracking channel width. The reason for the strong variation of results may stem from limitations of the test method used. Given that the flow visualization test rig only allows the preform impregnation on the top and bottom side of the preform to be monitored, it gives no insight into the filling pattern over the preform thickness and, therefore, no knowledge of the three-dimensional shape and volumetric size of the formed voids. Assuming an identical void volume, the shape of a void could vary between two extremes of a thin and wide shape and a high and narrow shape. Certain inhomogeneity during the preform impregnation could cause different void shapes of identical volume for experiments of the same race-tracking width leading to a varying observed area ratio of the void on the preform bottom side. Due to the use of a non-reactive fluid as flow media instead of reactive resins, the impregnated preform could not be cured and post-analyzed in order to inspect void volume and shape.

Comparing the experiment without a race-tracking channel in Figure 6a with the race-tracking experiments in Figure 6b,c, it is observed that the maximum recorded force at the end of the compression phase is reduced in the presence of a race-tracking channel. To further investigate this observation, the maximum recorded force for the three investigated scenarios is depicted in Figure 9 as dark blue bars as the mean value and with the standard deviation for three repetitions for each scenario. The results show that in the presence of a race-tracking channel, the mean of the maximum force is reduced by approximately 25%, and that there is statistically no difference between the two levels of race-tracking channel widths.

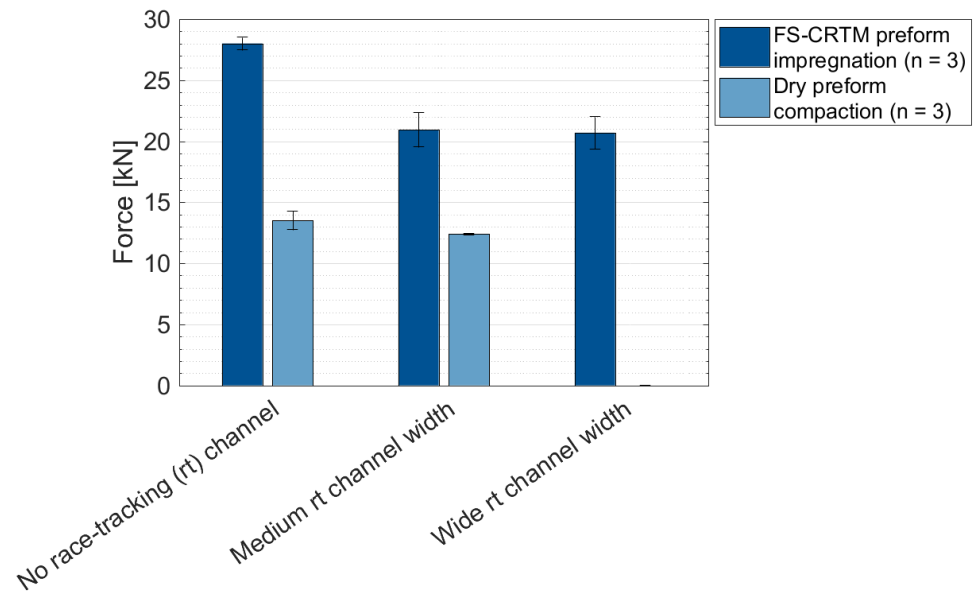


Figure 9. Maximum recorded force of the three experimental scenarios of the race-tracking study. Bar heights give the mean value, and the error bars indicate the standard deviation of three repetitions.

As previously mentioned, the one-dimensional laminate consolidation approach by Terzaghi [51] describes the recorded force during FS-CRTM impregnation experiments as a result of the combination of fluid pressure and preform compaction stress. While the preform compaction stress component is certainly changing due to the reduced preform dimensions, the fluid pressure component is assumed to be changing, too, due to an increased overall cavity porosity in the presence of an edge race-tracking channel. To investigate the change of these individual force components, additional experiments were performed for preforms without and with a medium race-tracking channel in which no

fluid was injected, which permitted the pure preform compaction force to be measured. The recorded maximum forces are shown in light blue in Figure 9, again showing mean values and the standard deviation for experiments completed in triplicate. Comparing the recorded forces for experiments without a race-tracking channel with experiments with a medium race-tracking channel width in Figure 9 indicates that the dry preform compaction force reduces only by approximately 1 kN, while the maximum force during FS-CRTM impregnation experiments is reduced by approximately 7 kN. Considering that the dry preform compaction is comparable to the wet preform compaction component during impregnation, these observations suggest that the reduction of the fluid pressure component is far larger than the preform compaction component in the presence of race-tracking. The strong reduction of the fluid pressure component is explained by two effects, which occur due the presence of edge race-tracking. First, the flow pattern changes from a predominant out-of-plane flow for experiments without a race-tracking channel to a superimposed flow with an additional lateral in-plane flow for experiments with race-tracking. The in-plane permeabilities of the used NCF material [44] are approximately one order of magnitude higher than its out-of-plane component, resulting in a reduced flow resistance during the lateral preform impregnation and an overall reduced fluid pressure. Second, the presence of a race-tracking channel increases the overall porosity inside the cavity, which reduces the fluid stagnation pressure at the end of the compression phase. Hence, flow pattern changes and increased cavity porosity leads to a strong reduction of fluid pressure which is seen to have caused the majority of the recorded force reduction in the presence of edge race-tracking.

3.2. Flow Control Study

Flow visualization experiments were performed during the flow control (FC) study to explore a passive flow control strategy to diminish the edge race-tracking effect during the FS-CRTM preform impregnation. The cavity in-plane dimensions were increased from 210×210 mm during the race-tracking (RT) study in the previous section to 228×228 mm in the presented FC study. This was necessary to realize an experimental scenario with a localized injection gap covering only the area under the central slider with 210×210 mm and circumferentially pre-compact the preform in the outer 9 mm of the cavity to the final part thickness. To explore the potential of a passive flow control strategy, experiments for three scenarios were again performed: without a race-tracking channel (indicated by an identifier with the test number, e.g., 'fcs-#1' for the first test) and with medium ('fcs-mrt-#1') and wide channel width ('fcs-wrt-#1').

Figure 10 illustrates overview plots of important process variables of the three experimental scenarios performed during the FC study. Due to the increased preform in-plane dimensions, the injected fluid volume was adapted, leading to a longer injection time for flow control experiments at an identical injection pressure to that during the RT study. All three experimental scenarios of the FC study in Figure 10a–c show a steep linear increase of the AFR of the preform top side, initiating at the process start. Due to mirroring effects, the top camera of the test rig could only record the fluid flow in the area of the central slider and not in the outer cavity section of the pre-compacted edge. Therefore, the reported AFR of the preform top side provides information only on the filling of the localized injection gap, which is seen to be completely filled before the injection is finished. The flow front progression on the preform top side is shown in Figure 11a,c,e. The herein shown filling pattern inside the injection gap progresses radially from the inlet slider ($x = 9$ mm, -20 mm $< y < 20$ mm) towards the vent side of the injection gap ($x = 219$ mm, -105 mm $< y < 105$ mm).

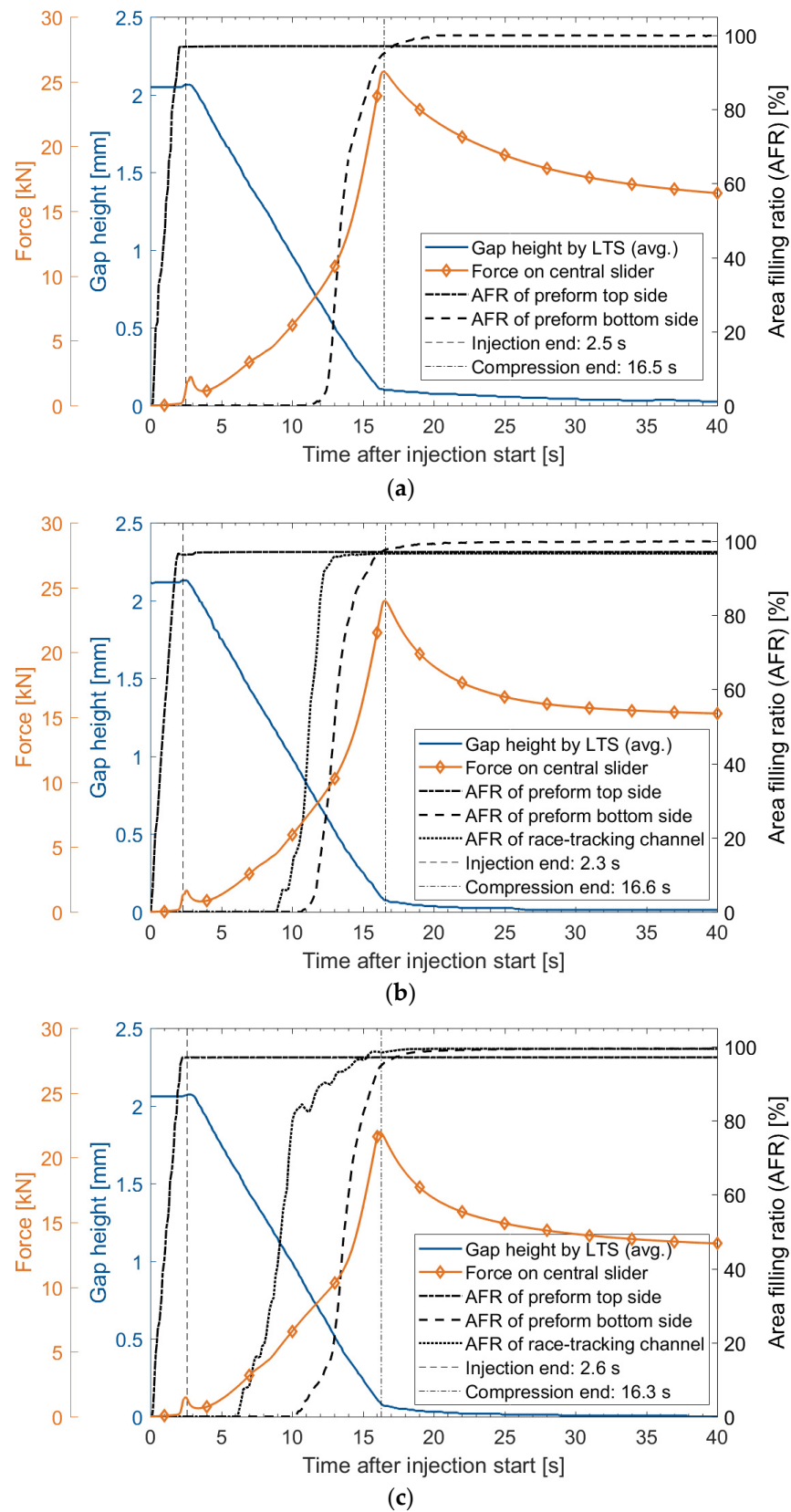


Figure 10. Overview of important process variables during FS-CRTM experiments of the flow control study: (a) no race-tracking channel—fcs-#1; (b) medium race-tracking channel width—fcs-mrt-#3; (c) wide race-tracking channel width—fcs-wrt-#2 (LTS = laser triangulation sensor).

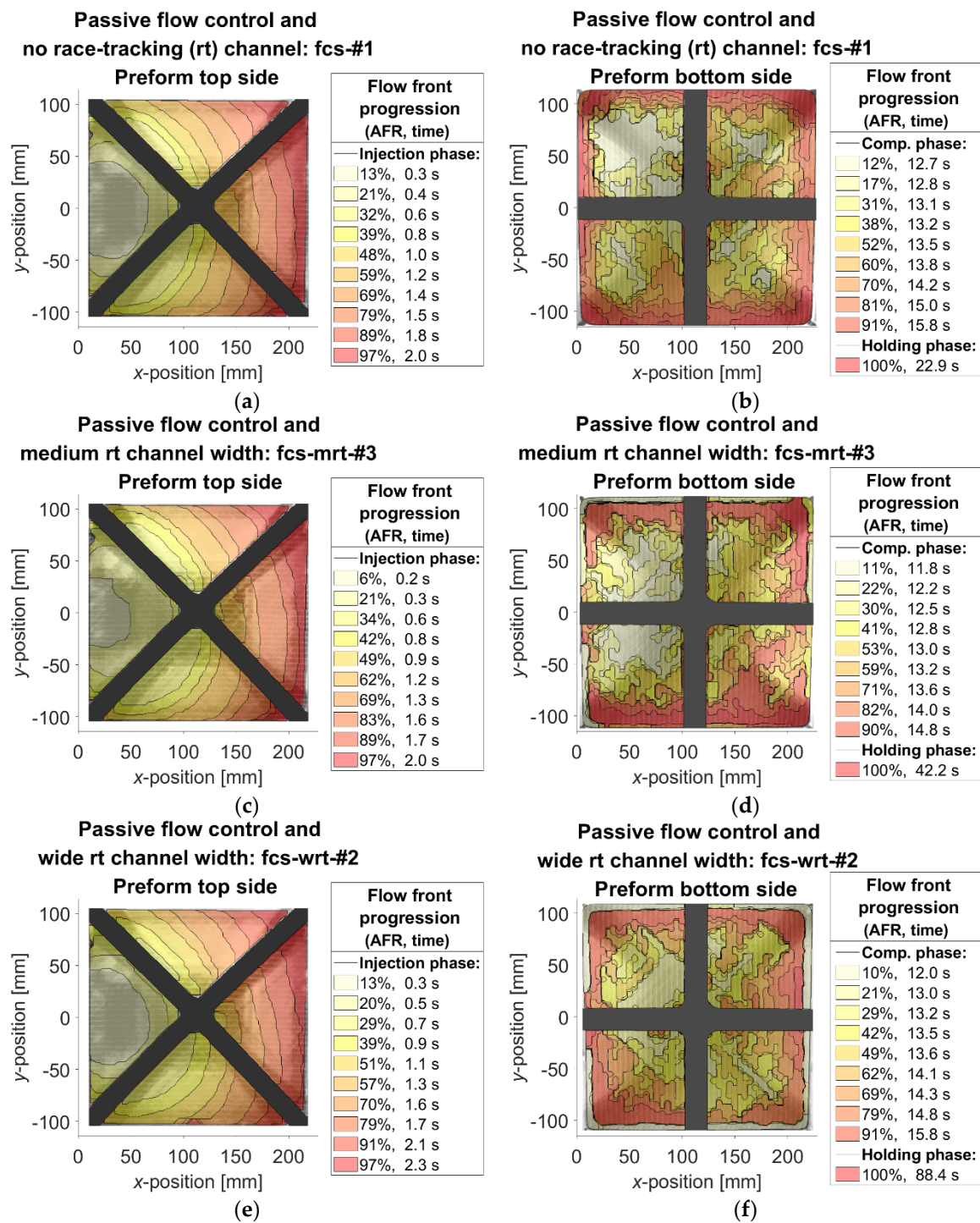


Figure 11. Flow front progression of FS-CRTM experiments of the flow control study: (a,b) no race-tracking (rt) channel—fcs-#1; (c,d) medium race-tracking channel width—fcs-mrt-#3; (e,f) wide race-tracking channel width—fcs-wrt-#2 (AFR = area filling ratio).

Similar to the experiments in the RT study, the force and gap height curve also increase at the end of the injection phase during the experiments of the flow control study (see Figure 10). The observed deflection of the curves is attributed to an increase in cavity pressure after the injection gap is completely filled, yet with remaining fluid being further injected. In contrast to the RT study, the force peaks during the FC study are reduced less when comparing the experiments without a race-tracking channel in Figure 10a and with a channel in Figure 10b,c. This observation is correlated to the fact that during the flow control

experiments, the fluid is injected into an isolated, central injection gap. Due to the applied passive flow control strategy, no direct spatial connection between the central injection gap and the edge race-tracking channel is established. Therefore, the presence of a race-tracking channel does not increase the empty space in which the fluid can discharge during the injection, which is identified as the cause for the peak reductions during the RT study.

As in the injection phase, the compression phase is also longer for experiments in the FC study compared to the RT study, due to the increased height of the injection gap at an identical closing speed of the central slider. During the recorded gap height reduction in Figure 10, the force applied to the central slider increases and peaks at the end of the compression phase before it relaxes during the holding phase. The maximum recorded force during the FC study is reduced in the presence of a race-tracking channel as previously observed and discussed during the RT study.

The dashed black line in Figure 10a shows the AFR of the preform bottom side of the flow control experiment without race-tracking. The AFR stays constant at zero until approximately 12 s after the process start and rises rapidly afterwards before the slope decreases towards full filling during the holding phase at approximately 23 s. Looking at the qualitative flow front progression on the preform bottom side of the same experiment in Figure 11b, it can be observed that the fluid fills the preform bottom side first in its center and then progresses towards the preform edges. These process observations in flow control experiments without race-tracking verify the intended flow manipulation of the passive flow control strategy to initiate a central through-thickness flow under the localized injection gap along with a subsequent lateral flow from the center towards the pre-compacted preform edge.

The initial rise of the AFR curve of the preform bottom side is defined as the 'time of initial through-thickness penetration' (TITTP). Figure 12 depicts in the two dark blue bars TITTP mean values and standard deviations for three experiments without a race-tracking channel for the RT study and the FC study. Considering a predominant out-of-plane flow in the preform center during the FC study, its TITTP should be comparable with the TITTP of the pure through-thickness impregnation of the RT study. Comparing the TITTP of the two studies in Figure 12, it is observed that the mean of the flow control experiments is slightly lower even though the injection time of this study is marginally longer by 0.4 s. The small extension of the injection phase during the flow control experiments seems to be compensated by a slightly faster out-of-plane flow due to the marginally lower areal weight of the fabric used for the FC study and the resulting lower preform thickness as recorded in Table A3 in Appendix A. Nevertheless, the injection time extension is very low compared to the absolute value of the TITTP. The identical preform architecture and the similarity in TITTP between the two studies strengthen the conclusion of the previous paragraph, i.e., a predominant out-of-plane flow is established in the preform center under the injection gap during the flow control experiments.

For experiments of the FC study, a faster progression until complete filling of the preform bottom side is recorded comparing the AFR of the preform bottom side of the FC study without a race-tracking channel in Figure 10a with the corresponding experiment of the RT study in Figure 6a. The observed difference of AFR progression on the preform bottom side is correlated to process design changes and resulting flow manipulations due to the applied passive flow control strategy in the FC study. While the TITTP of the two studies is comparable, the compression phase is longer in the FC study due to the increased height of the injection gap. This results in a longer remaining time span between TITTP and the compression end and in an increased gap height at TITTP for the flow control experiments compared to experiments of the RT study as shown in Figure 12. With the larger remaining gap height of the central slider at TITTP, more fluid is distributed between the arrival of the flow front on the preform bottom side and the end of the compression phase, filling the observed preform bottom side quickly from its center towards the edges as seen in Figure 11b.

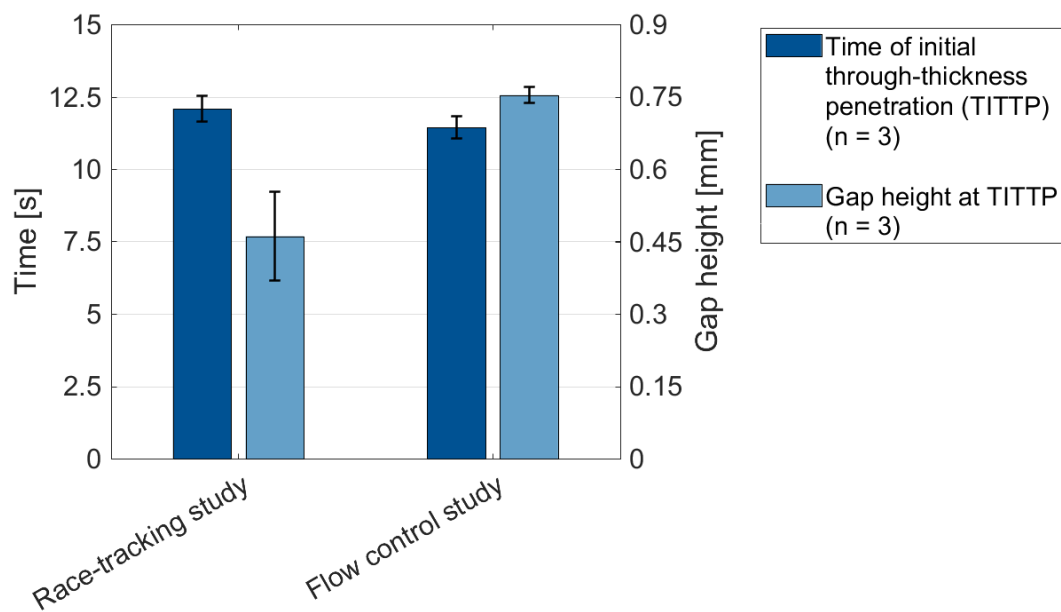


Figure 12. Time of initial through-thickness penetration (TITTP) and corresponding gap height of FS-CRTM experiments without a race-tracking channel from the race-tracking study and the flow control study. Shown are mean values and standard deviations for experiments in triplicate.

Observing the flow control experiments with a race-tracking channel in Figure 10b,c, the black dotted AFR curve of the race-tracking channel stays at zero during the complete injection phase and for parts of the compression phase until it rises rapidly. The delayed filling of the race-tracking channel is explained by the flow manipulation of the applied passive flow control strategy. Due to the spatial isolation of the central injection gap from the edge race-tracking channel, the flow has to pass through the pre-compacted preform edge before it fills the race-tracking channel, causing the observed time delay of the rise in the channel's AFR. On the contrary, the process design during the RT study provides a spatial connection between the injection gap and the race-tracking channel, resulting in an early filling of the race-tracking channel shortly after the injection start as seen in Figure 6b,c.

Comparing the flow control experiments with race-tracking in Figure 10b,c with each other, the rise in the AFR of the race-tracking channel is recorded as starting earlier for experiments with larger race-tracking channel widths. The rise at different times for different channel widths is caused, on the one hand, by the difference in preform dimensions and, on the other hand, by the specific flow pattern of the passive flow control strategy. All experiments of the FC study were performed at identical in-plane dimensions of the cavity and of the central slider realizing the injection gap. The race-tracking channel was created by cutting the centrally placed preform smaller than the in-plane dimensions of the cavity. Therefore, the width of the race-tracking channel defines the width of the pre-compacted preform edge. For a wider channel width, a resulting narrower pre-compacted preform edge section needs to be penetrated by the fluid, flowing from the central injection gap towards the race-tracking channel. Therefore, a shorter flow path leads to the observed earlier filling of the race-tracking channel with increased channel width as shown in Figure 10b,c.

Figure 11d,f shows the flow front progression on the preform bottom side for experiments of the FC study with medium and wide racetrack channel width, respectively. In both experiments, the out-of-plane flow under the central injection gap impregnates the preform bottom side from its center towards its edges, as previously discussed for the experiment without a race-tracking channel seen in Figure 11b. Additionally, the experiments with race-tracking in Figure 11d,f show a lateral flow from the race-tracking channel towards the preform center. Comparing these experiments with each other, the expansion of the lateral flow from the race-tracking channel towards the preform center increases with increasing channel width. On the one hand, this observation is explained by the earlier

filling of the race-tracking channel for increased channel width, as discussed in the previous paragraph. On the other hand, the lateral flow is promoted by the acting fluid pressure inside the race-tracking channel. Generally, the fluid pressure during the compression phase is caused by the closure movement of the central slider leading to a high fluid pressure inside the injection gap. Due to the spatial disconnection between the injection gap and the race-tracking channel, the fluid has to flow through the pre-compacted preform edge to fill the race-tracking channel. Thus, the developing fluid pressure inside the race-tracking channel is reduced by the porous preform edge that the fluid flows through. The wider the race-tracking channel width, the narrower the pre-compacted preform edge and the higher the developing fluid pressure inside the channel, causing the extended lateral flow as observed by comparing Figure 11d,f.

The flow front progression plot in Figure 11b shows that the outer corner sections of the preform are filled last on the preform bottom side in experiments without race-tracking in the FC study. This is explained by the filling pattern of the flow control experiments, i.e., first the area on the preform bottom side under the injection gap is filled, followed by a lateral penetration towards the edges. Due to the geometrical design of the square injection gap with a side length of 210 mm and corner radii of 10 mm and of the square cavity with a side length of 228 mm and corner radii of 10 mm, the distances between the radii of the injection gap and cavity are the largest, and therefore, the outer preform corner sections are the last to be filled. The filling pattern overview of the flow control experiments with a race-tracking channel in Figure 11d,f is not clear on this matter, for which reason additional flow front images are presented in Figure 13. The pictures show the preform bottom side at the time of complete filling at 23 s of the experiment without race-tracking in Figure 13a and the corresponding pictures of experiments with a medium and wide race-tracking channel at the same point in time in Figure 13b,c. The complete preform impregnation of the preform is delayed for experiments with race-tracking, observable by the unimpregnated preform sections in their corners. In contrast to the experiment without race-tracking, the sections filled last are not at the outer edge of the corner but located slightly inside the preform, entrapped between the two merging flows from the preform center and from the race-tracking channel.

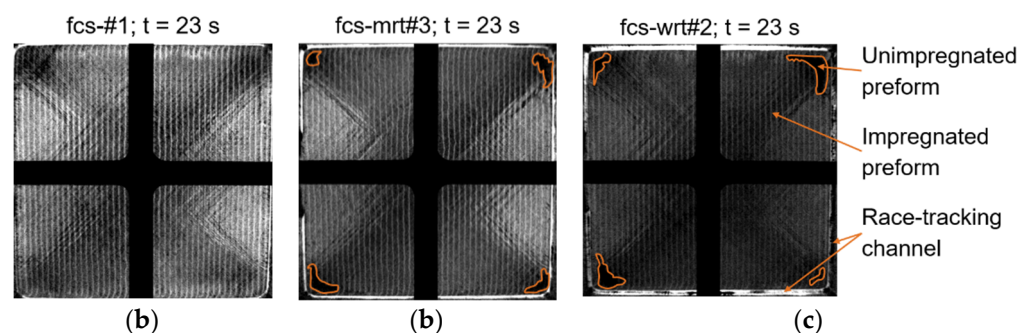


Figure 13. Preform impregnation on the bottom side of the three experimental scenarios of the flow control study at 23 s: (a) complete filling of experiment without a race-tracking channel fcs-#1; unimpregnated corner sections of experiments with a medium fcs-mrt#3 (b) and wide fcs-wrt#2 (c) race-tracking channel.

A shift of the location of the lastly filled preform section is observed by comparing the flow control experiments with race-tracking with the corresponding experiments performed during the RT study. While the experiments of the RT study consistently show the lastly filled section in the center of the preform, the manipulated flow due to the passive flow control strategy of the FC study relocates the lastly filled section towards the outer preform corners. This is traced back to the process design changes, which spatially disconnected the central injection gap from the edge race-tracking channels and initiate a preform impregnation from the preform center towards its edges. Therefore, the lastly filled preform sections and potential macro voids due to edge race-tracking are shifted

towards the outer preform corners in experiments of the FC study. Manipulating the flow to locate potential manufacturing flaws, such as macro voids, at the edge section of the manufactured part, which is generally machined off, decreases the risk of scrapped parts and highlights once more the benefit of the investigated passive flow control strategy for a robust FS-CRTM production.

4. Summary and Conclusions

In this paper, flow visualization experiments for the film-sealed compression resin transfer molding (FS-CRTM) process have been presented. Two studies were performed to investigate: (i) the effect of edge race-tracking and (ii) a passive flow control strategy to diminish edge race-tracking. Through the experimental observations, typical flow propagation scenarios are derived describing the impregnation of preforms of small geometrical aspect ratios without and with race-tracking as well as during the application of the investigated passive flow control strategy.

Figure 14a illustrates the first-derived scenario of the preform impregnation during the FS-CRTM process without edge race-tracking. The observations from the flow visualization experiments revealed a fast distribution of fluid above the top preform surface inside the injection gap, which is fully filled during the injection phase. The tool closure movement during the compression phase initiates an out-of-plane flow propagation nearly parallel to the top preform surface. The out-of-plane flow was observed by a delayed arrival of the flow front on the preform bottom side. The general flow of the derived FS-CRTM scenario correlates with other studies in the technical literature for the conventional CRTM process of preforms with small geometrical aspect ratios [7,8,40].

The second-derived flow scenario of the FS-CRTM preform impregnation in the presence of edge race-tracking is shown in Figure 14b. During the injection phase, the early filling of the injection gap is observed to be accompanied by the filling of the race-tracking channel due to their spatial connection. Based on the observations made, the preform impregnation during the compression phase is concluded to consist, in simplified terms, of three flow regions as illustrated in Figure 14b. In region 1, at the edge of the preform, a predominant in-plane flow develops from the race-tracking channel towards the preform center. In region 3, at the center of the preform, furthest away from the race-tracking channel, an undisturbed, predominant out-of-plane flow is established from the preform top towards the bottom side. In region 2, the transition region, a superimposed flow of the neighboring in-plane and out-of-plane flows is developed. The derived flow scenario demonstrates the change of flow pattern during the FS-CRTM preform impregnation in the presence of edge race-tracking caused by the additional lateral in-plane flow from the race-tracking channel towards the center of the preform. The described flow scenario in the presence of edge race-tracking correlates well with numerical simulations of the conventional CRTM process presented in [40].

The experiments of the race-tracking (RT) study show that a FS-CRTM process design in which the fluid is injected into an injection gap that covers the complete preform top surface is very sensitive to edge race-tracking. The direct spatial connection between the injection gap and the race-tracking channel leads to an early filling of the race-tracking channel and a subsequent lateral in-plane flow from the race-tracking channel to the center of the preform. Considering that the in-plane permeabilities of a reinforcement structure are generally one order of magnitude higher than its out-of-plane permeability, the lateral in-plane flow will always significantly penetrate the preform before the out-of-plane flow saturates the preform in the through-thickness direction. As a result, macro void formation occurs, which was observed in all experiments with race-tracking during the RT study. In industrial production, such flaws lead to non-compliance of quality requirements (i.e., mechanical performance and surface quality) and require parts to be scrapped, which needs to be avoided.

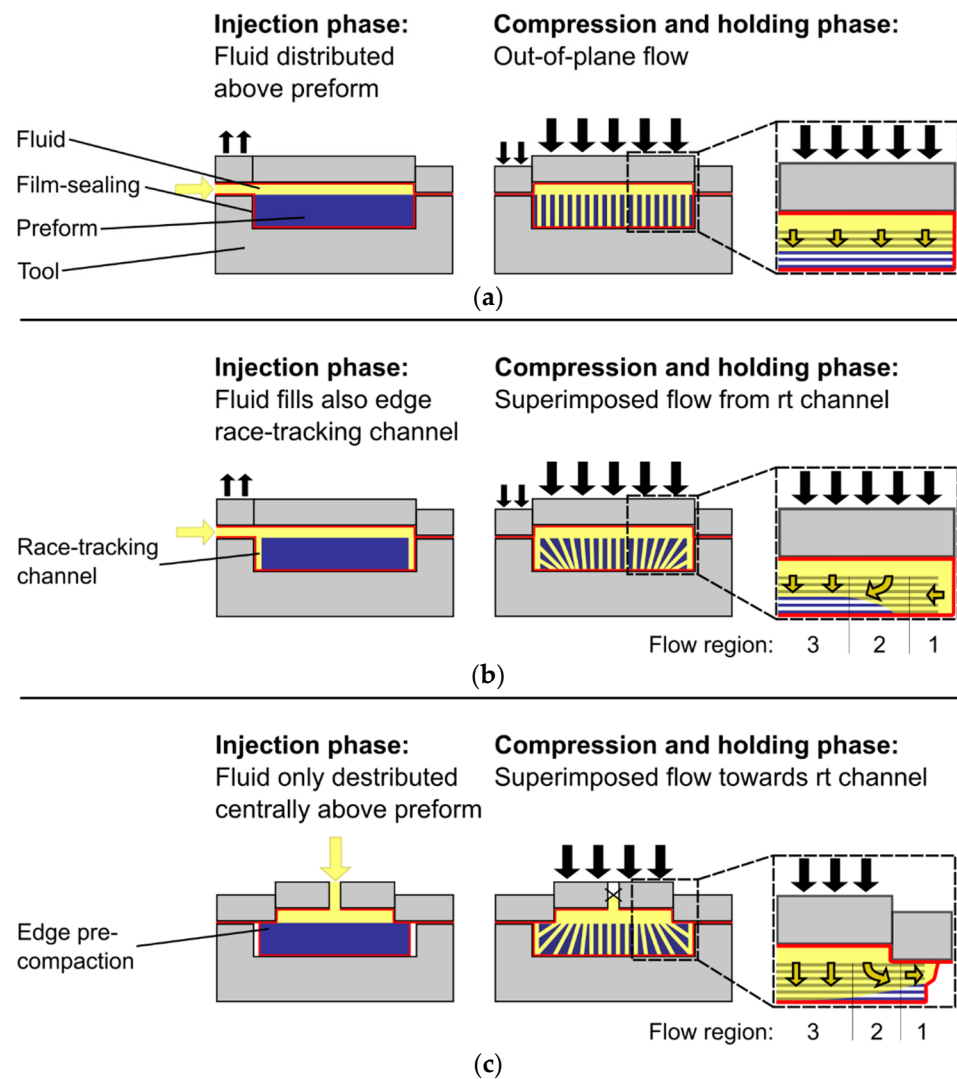


Figure 14. Flow scenarios derived from FS-CRTM experiments: (a) without edge race-tracking (rt) channel; (b) with edge race-tracking channel; and (c) with applied passive flow control strategy of a localized, central injection gap and pre-compaction of the preform edge.

The investigated passive flow control strategy provides a solution to diminish the edge race-tracking effect and increases the process robustness of the FS-CRTM process. Specifically, employed design changes manipulate the flow progression as shown in the third simplified flow scenario in Figure 14c. During the injection phase, the fluid is distributed inside a localized injection gap. The injection gap spans only over the central preform section and is disconnected from a potential edge race-tracking channel by the pre-compacted outer preform edge. During the compression phase, a preform impregnation is initiated from the preform center towards its edges. The flow pattern, due to the applied passive flow control strategy, is simplified, described in three flow regions as illustrated in Figure 14c. The closure of the central slider above the injection gap promotes a predominant out-of-plane impregnation in the central preform section of flow region 3. In the neighboring region 2, the flow is transferred towards a predominant in-plane flow in the outer part of the pre-compacted preform edge of region 1. Therefore, a superimposed flow is established in region 2 but now manipulated to flow from the preform center of the preform towards its edge, filling a potential edge race-tracking channel late in the process. The observed manipulated flow pattern of the passive flow control strategy correlates well with numerical CRTM simulations in [40].

In the presence of a race-tracking channel, the experiments with an applied passive flow control strategy revealed that a lateral in-plane flow from the race-tracking channel towards the center of the preform is still developed but to a reduced extent compared to experiments without the passive flow control strategy. The reduction of the lateral flow is caused by the difference in process design between the two studies. For the process design in the RT study (without a passive flow control strategy), the injection gap and the edge race-tracking channel are spatially connected. This results, on the one hand, in an early filling of the race-tracking channel and, on the other hand, in a homogeneous pressure field between the fluid in the injection gap and the fluid inside the race-tracking channel. The consequences are an early start of a lateral preform impregnation and a fast lateral flow progression due to the large fluid pressure increase during the compression phase. For the process design in the flow control (FC) study, the injection gap and the edge race-tracking channel are spatially disconnected due to the applied passive flow control strategy. Therefore, the fluid needs to flow through the pre-compacted preform edge before it fills the race-tracking channel. The delayed filling of the race-tracking channel results in a reduced time span in which the lateral race-tracking flow can penetrate the preform. Additionally, the pre-compacted preform edge acts as a pressure reducer between the high fluid pressure inside the injection gap and the adjusted, lower fluid pressure inside the race-tracking channel. The lowered fluid pressure inside the race-tracking channel leads to a reduced lateral flow propagation observed during the FC study. Therefore, comparison of the two studies emphasizes the effectiveness of the passive flow control strategy to diminish the edge race-tracking effect during the preform impregnation of the FS-CRTM process.

Besides changes in the flow pattern, edge race-tracking is identified as cause for a force reduction of up to 25% recorded at the central slider, which is directly correlated to the cavity pressure. The reduced cavity pressure during the tool closure is considered to be caused by the change from a pure out-of-plane to a superimposed preform impregnation with sections of out-of-plane and in-plane flow. Considering that in-plane permeabilities are generally one order of magnitude higher than the out-of-plane permeability of reinforcement structures, the developed fluid pressure during the preform impregnation reduces in the presence of edge race-tracking. The reduction of the stagnation pressure at the end of the compression phase is explained by an increased overall porosity inside the cavity in the presence of a race-tracking channel resulting from the reduced preform in-plane dimensions. Furthermore, a drop in the final stagnation pressure is also recorded for experiments with an applied passive flow control strategy and is therefore purely dependent on the existence of an edge race-tracking channel, and not on the preform impregnation pattern during FS-CRTM.

The presented paper is an important step toward comprehensively understanding and controlling the preform impregnation during FS-CRTM processing. The studies show that: (i) edge race-tracking significantly alters the impregnation pattern of preforms of a small geometrical aspect ratio (50), and (ii), importantly, that the passive flow control strategy is an effective solution to diminish the race-tracking effect and realize a more robust FS-CRTM process. Nevertheless, despite these promising results, future research is needed to study the edge race-tracking of preforms of a large preform aspect ratio (>100) in which the injection gap is not completely filled before the tool is in contact with the preform [8,9]. Additionally, a reduction of gap height is expected to strongly alter the flow pattern in the presence of edge race-tracking due to a reduced ratio of (equivalent) permeabilities between: (i) injection gap and race-tracking channel as well as (ii) injection gap and preform. The reduced permeability ratios are anticipated to result in a more complicated preform impregnation pattern due to a potential advancing in-plane flow of the fluid inside the race-tracking channel during tool closure and after the tool is in contact with the preform, similar to the race-tracking flow during the conventional RTM process.

The presented results are also a starting point for developing and validating models to simulate the film integration into the CRTM process and the edge race-tracking effect during FS-CRTM processing. Hereby, industrial process designs can virtually and cost-effectively be validated for their robustness towards edge race-tracking in an early development phase. Furthermore, the present paper validates the approach of film-sealing the injection space inside the tool to enable a seal-free tool design for fiber reinforced plastic (FRP) production. Exploiting the benefits of film-sealed preforms, slider tooling technology was used to passively manipulate the fluid flow during FS-CRTM preform impregnations. In future work, slider tooling designs may enable automated FRP production via the FS-CRTM process of complex part geometries with, for example, undercuts that are currently produced via labor-intensive processes involving manually placing and removing inserts for each produced part.

Author Contributions: Conceptualization, M.V., S.Z., P.M. and K.D.; methodology, M.V.; validation, M.V.; formal analysis, M.V.; investigation, M.V.; resources, M.V. and S.Z.; data curation, M.V.; writing—original draft preparation, M.V.; writing—review and editing, M.V., S.Z. and P.M.; visualization, M.V.; supervision, M.V., S.Z., P.M. and K.D.; project administration, M.V.; funding acquisition, M.V., S.Z. and K.D. All authors have read and agreed to the published version of the manuscript.

Funding: This research was funded by the German Federal Ministry for Economic Affairs and Energy (BMWi), grant number ZF4004314TA9.

Acknowledgments: The work in this paper is based on research done for the project ‘SKR-FVK—Steigerung der Kosteneffizienz und Robustheit in der automatisierten Produktion faserverstärkter Kunststoffbauteile’. The authors thankfully acknowledge the funding of the BMWi and the contribution of all project partners enabling the success of the ongoing project SKR-FVK: Alpex Technologies GmbH, DEKUMED Kunststoff- und Maschinenvertrieb GmbH & Co. KG, RAC GmbH—Riedmann Advanced Composite, Polymer Competence Center Leoben GmbH, and Chair of Carbon Composites—Technical University of Munich. Final thanks go to the technicians and students of the Chair of Carbon Composites, Technical University of Munich, who supported the development of the experimental setup—R. Rauch, J. Kil, R. Ernhofer, M. Schreiber, H. Baumann, A. Prenninger, and P. Laubichler—and helped during sample as well as experiment preparation—D. Amrein, J. Stockbauer, and T. Erschbaumer.

Conflicts of Interest: The authors declare no conflict of interest.

Appendix A

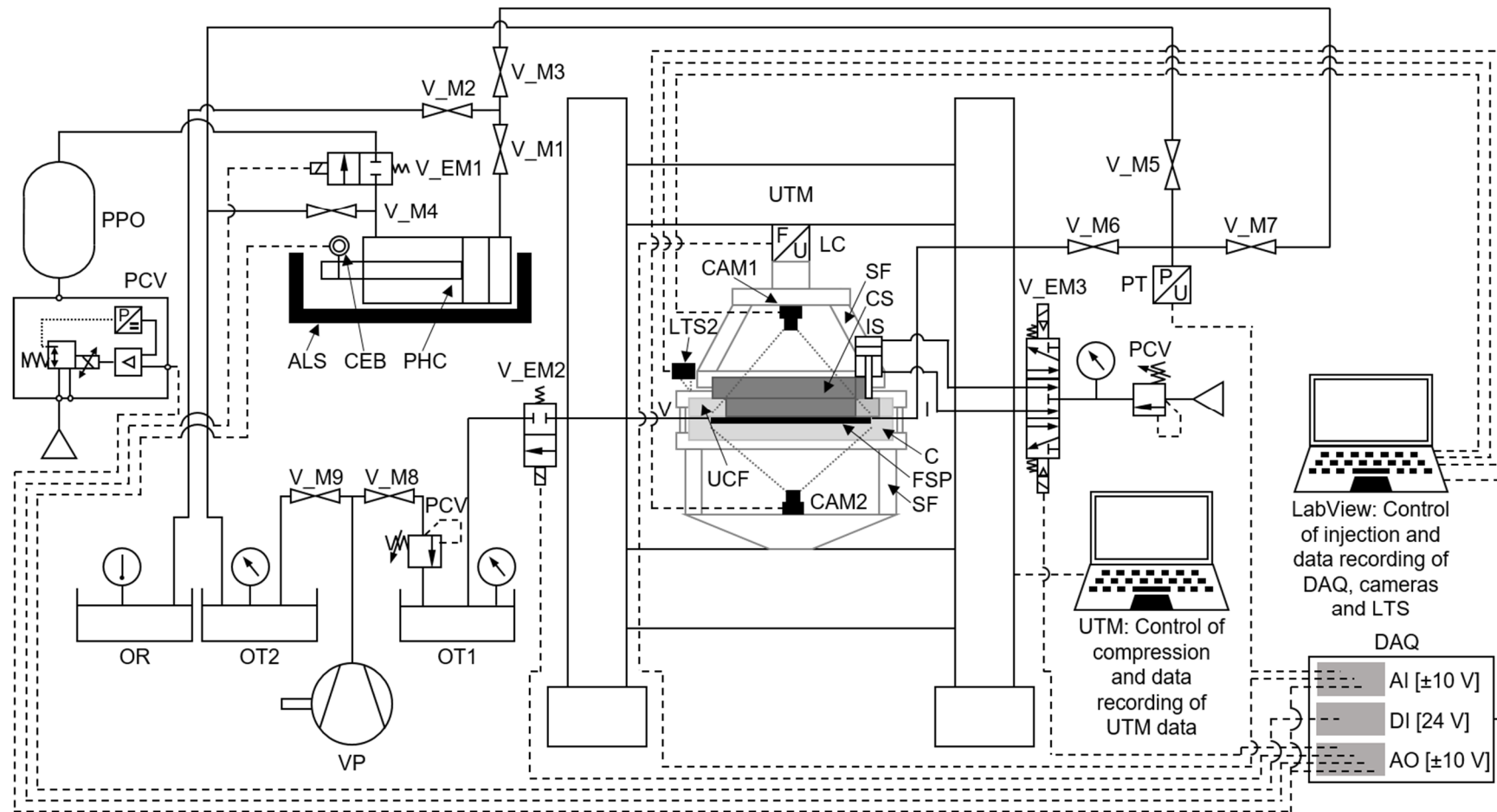


Figure A1. Schematic of flow visualization test rig. For a list of abbreviations and further details, see Table A1.

Table A1. List of abbreviations and further details on flow visualization setup of Figure A1.

Abbreviation	Equipment Description	Manufacturer	Type
ALS	Adjustable limit stop	-	-
AI	Analogue input	National Instruments	NI 9201
AO	Analogue output	National Instruments	NI 9236
C	Cavity (optically transparent)	-	-
CAM1/2	Industrial cameras with fisheye lens	- CAM1/2: The Imaging Source - Lens: Computar	- CAM1: DMK 22AUC03 - CAM2: DMK 27AUR0135 - Lens: T2314FICS-3
CEB	Converter-empty button	-	-
CS	Central slider (optically transparent)	-	-
DAQ	Data acquisition unit	National Instruments	NI cDAQ™-9174
DI	Digital input	National Instruments	NI 9421
FSP	Film-sealed preform package	-	-
I	Inlet	-	-
IS	Inlet slider including actuator	Actuator: Riegler	- Actuator: Kompaktzylinder LINER according to ISO 21287 Ø 80 250 kN (10-003-327)
LC	Load cell	Hegewald & Peschke	optoNCDT ILD1302-50
LTS1/2	Laser triangulation sensor	Micro-Epsilon	-
OR	Oil reservoir	-	-
OT1/2	Oil trap	-	-
PCV	Pressure control valve	IMI Norgren	VP5010BJ111H00
PHC	Pneumatic-hydraulic converter	Riegler	Zylinder ISO 15552 Ø 32–125 mm
PPO	Pressure pot	Airtech	-
PT	Pressure transducer	Gems	Psibar 1200 Series
SF	Stiffening structure	-	-
UCF	Upper cavity frame	-	-
UTM	Universal testing machine	Hegewald & Peschke	Inspekt 250 kN
V	Vent	-	-
V_M1—9	Manual valves	-	-
V_EM1—3	Electromagnetic valves	- V_EM1: AirTAC - V_EM2: ODE - V_EM3: METAL WORK	- V_EM1: 2W050-15 - V_EM2: 21A2KT30 - V_EM3: 7010022200
VP	Vacuum pump	Oerlikon Leybold Vacuum	TRIVAC D25BCS

Table A2. Preform data and resulting theoretical race-tracking channel width (neglecting preform placement tolerances).

Experiment	Preform Weight	Preform Length (Including Transition Zone for Race-Tracking Experiments)	Preform Width	Theoretical Race-Tracking Channel on Inlet Side	Theoretical Race-Tracking Channel on Vent Side	Theoretical Lateral Race-Tracking Channels
[-]	[g]	[mm]	[mm]	[mm]	[mm]	[mm]
vc-#1	213.2	211.1	210.5	-	-	-
vc-#2	213.2	211.1	210.5	-	-	-
vc-#3 ¹	212.0	211.2	210.6	-	-	-
mrt-#1	205.6	209.2	206.4	1.9	0.6	1.7
mrt-#2	205.5	209.4	206.7	1.8	0.4	1.6
mrt-#3	205.2	209.4	206.6	2.2	0.4	1.6
wrt-#1	197.9	207.5	202.7	4.2	2.3	3.5
wrt-#2	198.0	207.2	202.7	4.0	2.6	3.6
wrt-#3	199.2	206.2	202.6	3.8	1.7	3.6
fcs-#1	245.4	228.0	228.3	-	-	-
fcs-#2	245.6	228.1	228.1	-	-	-
fcs-#3	245.8	228.0	228.1	-	-	-
fcs-mrt-#1	237.6	226.1	224.2	2.0	1.7	1.8
fcs-mrt-#2	237.2	226.2	224.0	2.1	1.7	1.9
fcs-mrt-#3	237.1	225.9	223.8	2.0	1.9	2.0
fcs-wrt-#1	230.3	223.9	219.9	3.9	3.9	4.0
fcs-wrt-#2	229.6	223.8	220.0	3.9	4.0	3.9
fcs-wrt-#3	229.8	224.0	219.9	4.2	4.0	4.0
dryComp-#1	210.8	211.1	210.4	-	-	-
dryComp-#2	210.7	211.4	210.3	-	-	-
dryComp-#3 ¹	212.0	211.2	210.6	-	-	-
dryComp-mrt-#1	205.7	209.1	206.5	1.9	0.7	1.7
dryComp-mrt-#2	205.7	209.4	206.4	2.1	0.4	1.7
dryComp-mrt-#3	205.2	208.9	206.6	1.9	0.9	1.6

¹ Same preform was used for dry compaction, dryComp-#3, and FS-CRTM impregnation, vc-#3. During the film-sealing process and preparatory work prior to each experiment, all preforms were compacted five times under vacuum pressure. The literature [52] shows that elastically repeatable deformation is reached after the third compaction cycle. Therefore, it was assumed that the extra cycle of dry compaction of this preform would not change the FS-CRTM process, which has been proven by the comparable maximum force levels of experiments vc-#1, vc-#2, and vc-#3.

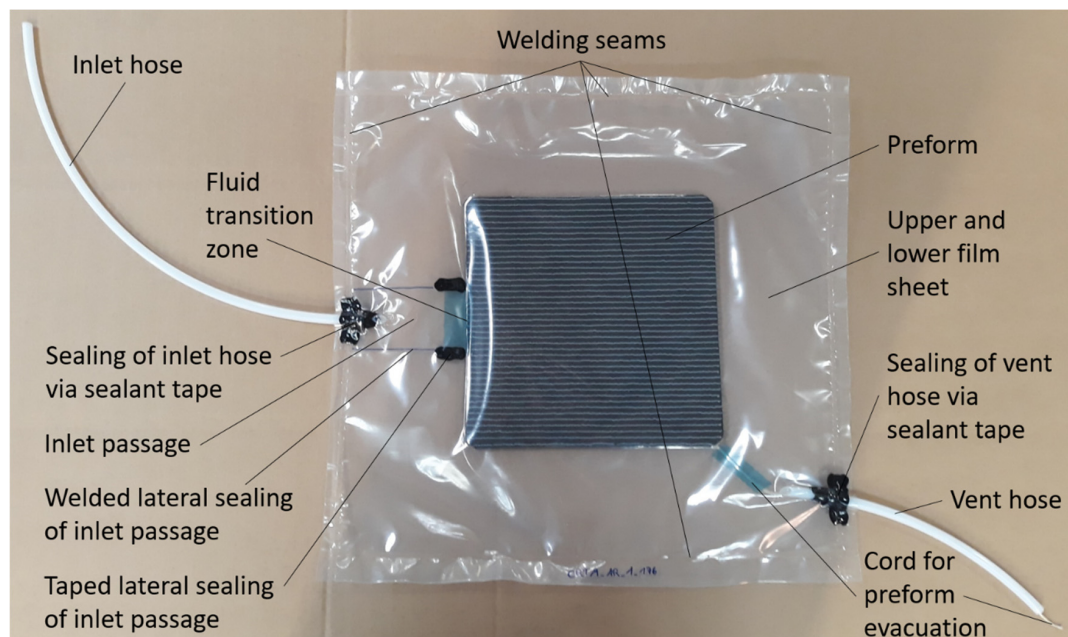


Figure A2. Features and components of a film-sealed preform package.

Table A3. Process factors of the presented experiments.

Experiment	Preform Thickness at Vent Pressure ¹	Viscosity of Oil ²	Pot Pressure ^{3,4}	Stagnation Pressure ^{3,5}	Vent Pressure ³	Height of Injection Gap
[-]	[mm]	[mPa.s]	[kPa]	[kPa]	[kPa]	[mm]
vc-#1	5.0 ± 0.1	49.9	368.2 ± 1.1	293.6	-90.0	1.41
vc-#2	5.1 ± 0.0	49.9	368.4 ± 1.1	295.9	-90.0	1.42
vc-#3	5.0 ± 0.0	51.0	368.2 ± 1.0	297.0	-90.0	1.40
mrt-#1	5.0 ± 0.0	49.8	368.5 ± 1.1	294.4	-90.0	1.40
mrt-#2	5.0 ± 0.0	49.8	368.2 ± 1.1	297.0	-90.0	1.40
mrt-#3	4.9 ± 0.1	49.5	368.4 ± 1.1	296.7	-89.9	1.41
wrt-#1	5.0 ± 0.1	49.9	368.5 ± 1.1	298.2	-90.0	1.41
wrt-#2	4.9 ± 0.1	49.9	368.0 ± 1.1	297.7	-89.9	1.40
wrt-#3	5.0 ± 0.1	49.5	368.6 ± 1.0	298.7	-90.0	1.39
fcs-#1	4.8 ± 0.0	51.1	367.9 ± 1.2	295.2	-90.0	1.55
fcs-#2	4.8 ± 0.0	50.0	368.0 ± 1.2	293.9	-90.0	1.54
fcs-#3	4.9 ± 0.1	50.7	368.1 ± 1.2	294.0	-90.0	1.55
fcs-mrt-#1	4.8 ± 0.1	50.3	368.0 ± 1.1	294.1	-90.0	1.54
fcs-mrt-#2	4.8 ± 0.1	51.1	367.9 ± 1.2	293.6	-90.0	1.56
fcs-mrt-#3	4.9 ± 0.0	50.7	367.8 ± 1.2	296.9	-90.0	1.54
fcs-wrt-#1	4.9 ± 0.1	50.9	368.0 ± 1.2	293.9	-90.0	1.54
fcs-wrt-#2	4.8 ± 0.1	50.3	367.9 ± 1.2	297.4	-90.0	1.54
fcs-wrt-#3	4.8 ± 0.1	50.9	367.9 ± 1.2	294.7	-90.0	1.55

¹ Mean and standard deviation measured at four points of the preform. ² Based on the measured oil temperature of the experiment, the viscosity was measured with a cone-plate measuring system on a Modular Compact Rheometer (MCR) 302 of Anton Paar (Graz, Austria) at a shear rate of 100 s⁻¹. ³ Differential value relative to ambient pressure. ⁴ Mean and standard deviation measured during the injection phase of the experiment. ⁵ Measured by pressure transducer in feeding line of inlet before injection start.

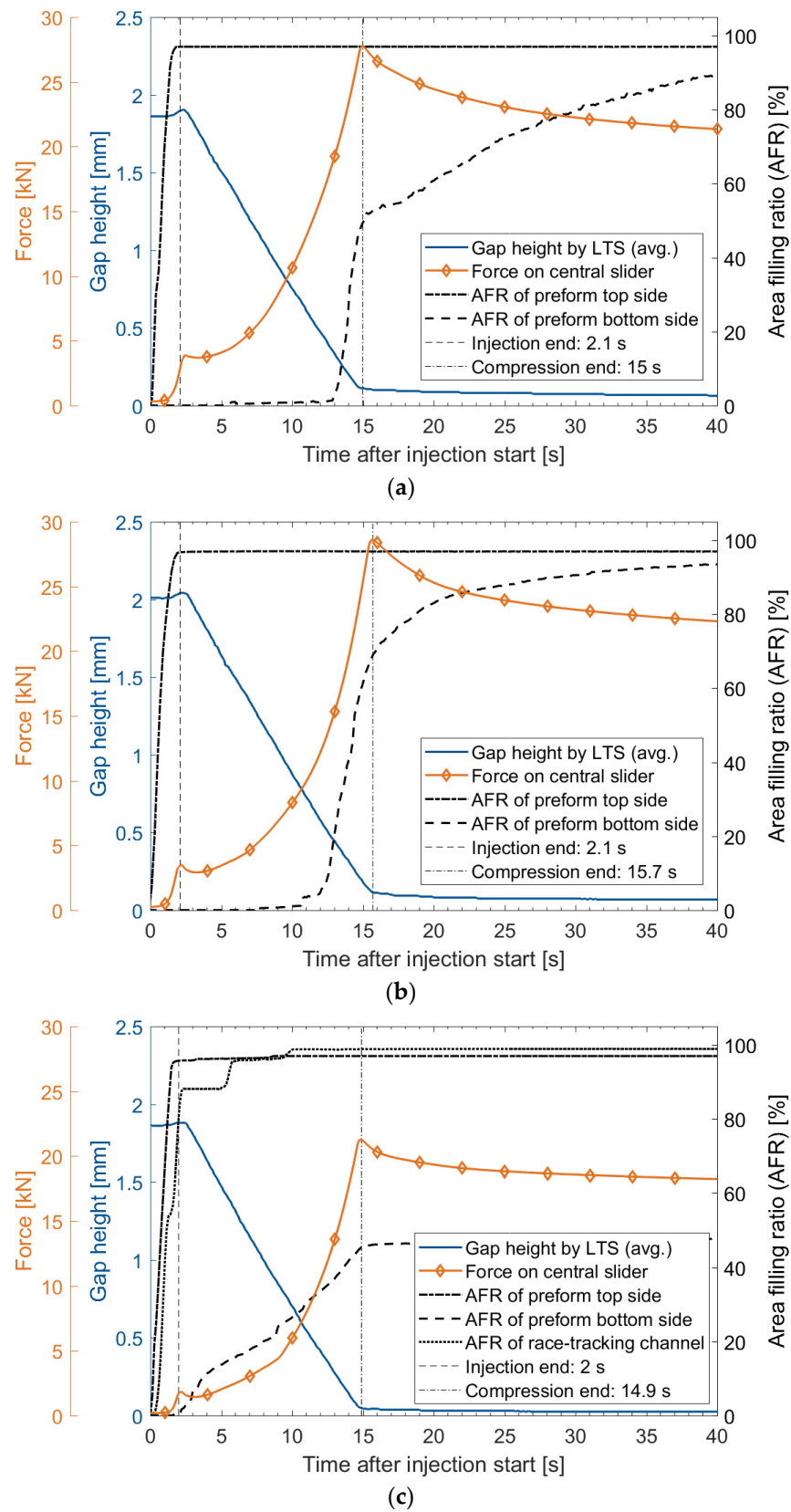


Figure A3. Overview of important process variables during FS-CRTM experiments of the race-tracking study: (a) no race-tracking channel—vc-#1; (b) no race-tracking channel—vc-#2; (c) medium race-tracking channel width—mrt-#1 (LTS = laser triangulation sensor).

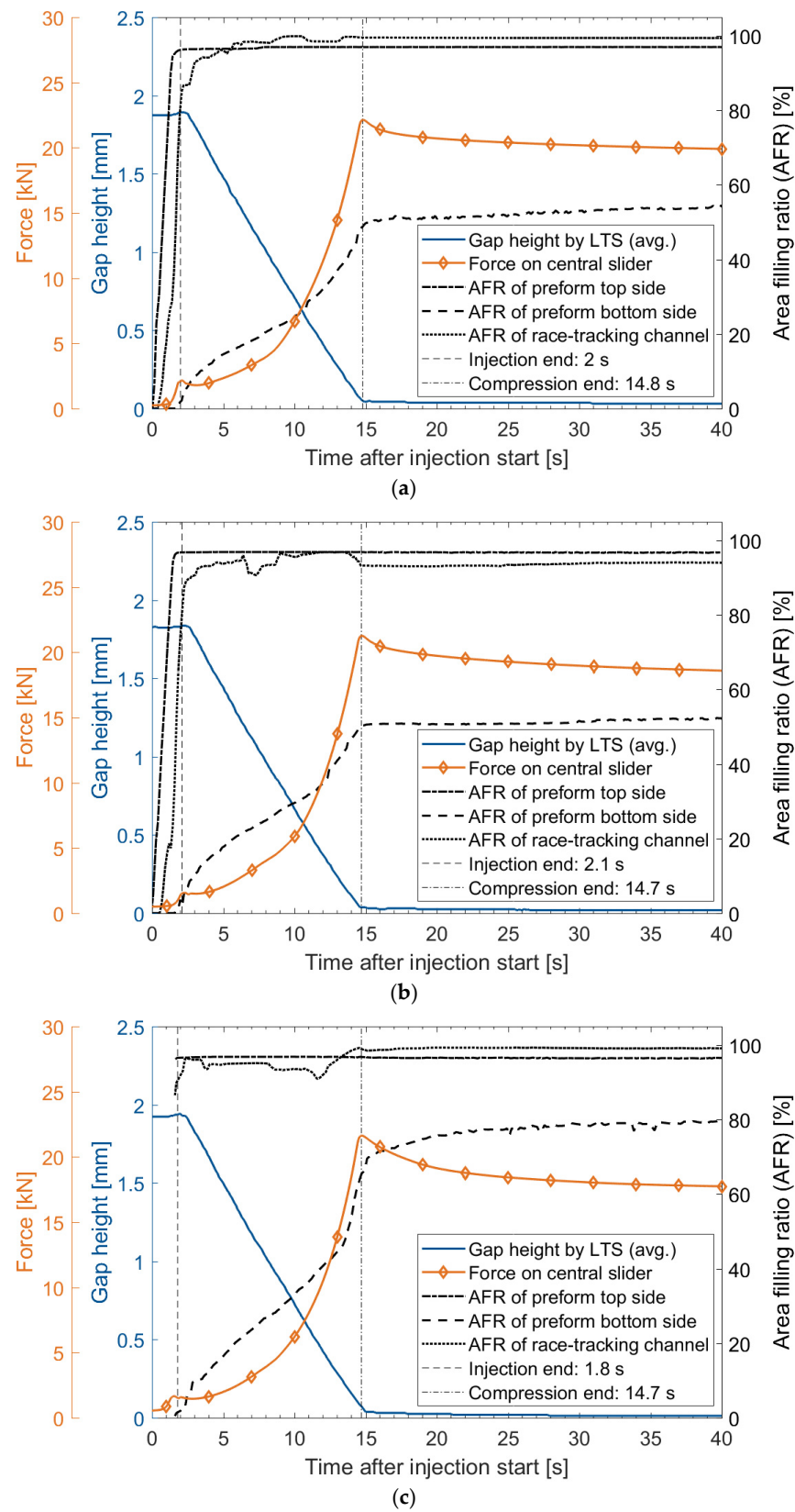


Figure A4. Overview of important process variables during FS-CRTM experiments of the race-tracking study: (a) medium race-tracking width—mrt-#2; (b) wide race-tracking width—wrt-#2; (c) wide race-tracking width—wrt-#3—no pictures of the preform top side were recorded during the injection of wrt-#3 due to issues of the data acquisition equipment (LTS = laser triangulation sensor).

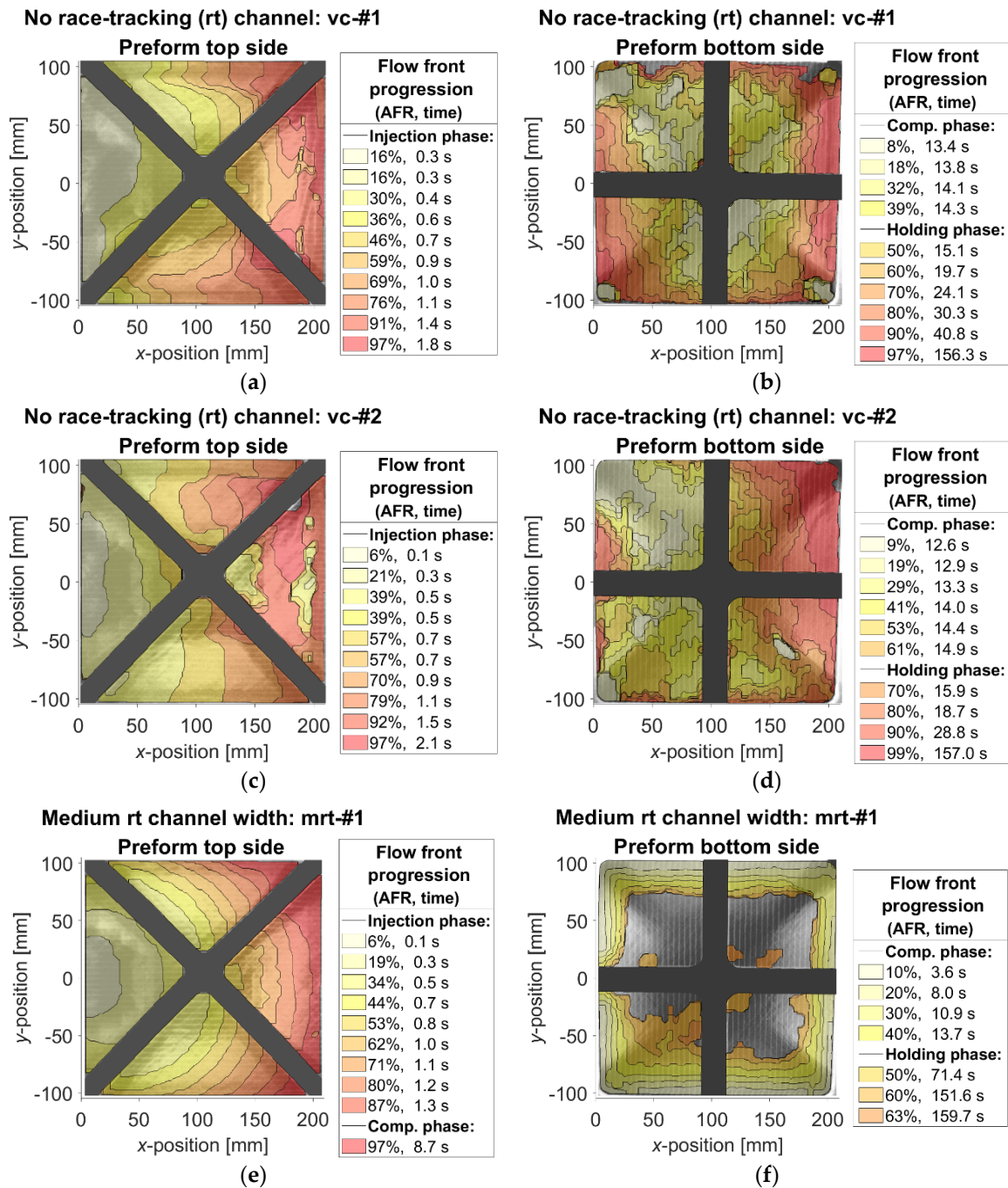


Figure A5. Flow front progression of FS-CRTM experiments of the race-tracking study: (a,b) no race-tracking (rt) channel—vc-#1; (c,d) no race-tracking channel—vc-#2; (e,f) medium race-tracking channel width—mrt-#1 (AFR = area filling ratio).

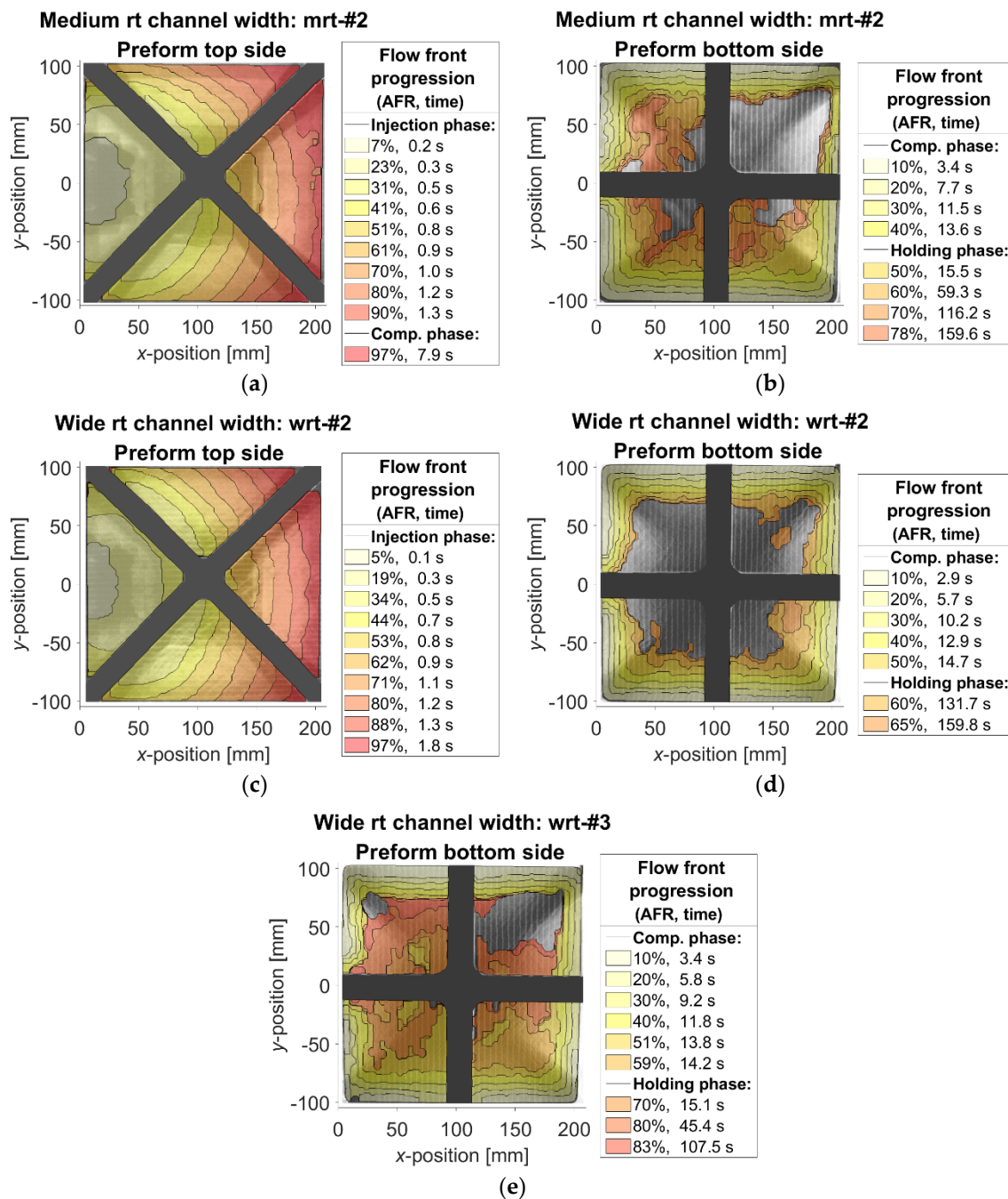


Figure A6. Flow front progression of FS-CRTM experiments of the race-tracking study: (a,b) medium race-tracking (rt) channel width—mrt-#2; (c,d) wide race-tracking channel width—wrt-#2; (e) wide race-tracking channel width—wrt-#3—no pictures of the preform top side were recorded during the injection of wrt-#3 due to issues of the data acquisition equipment (AFR = area filling ratio).

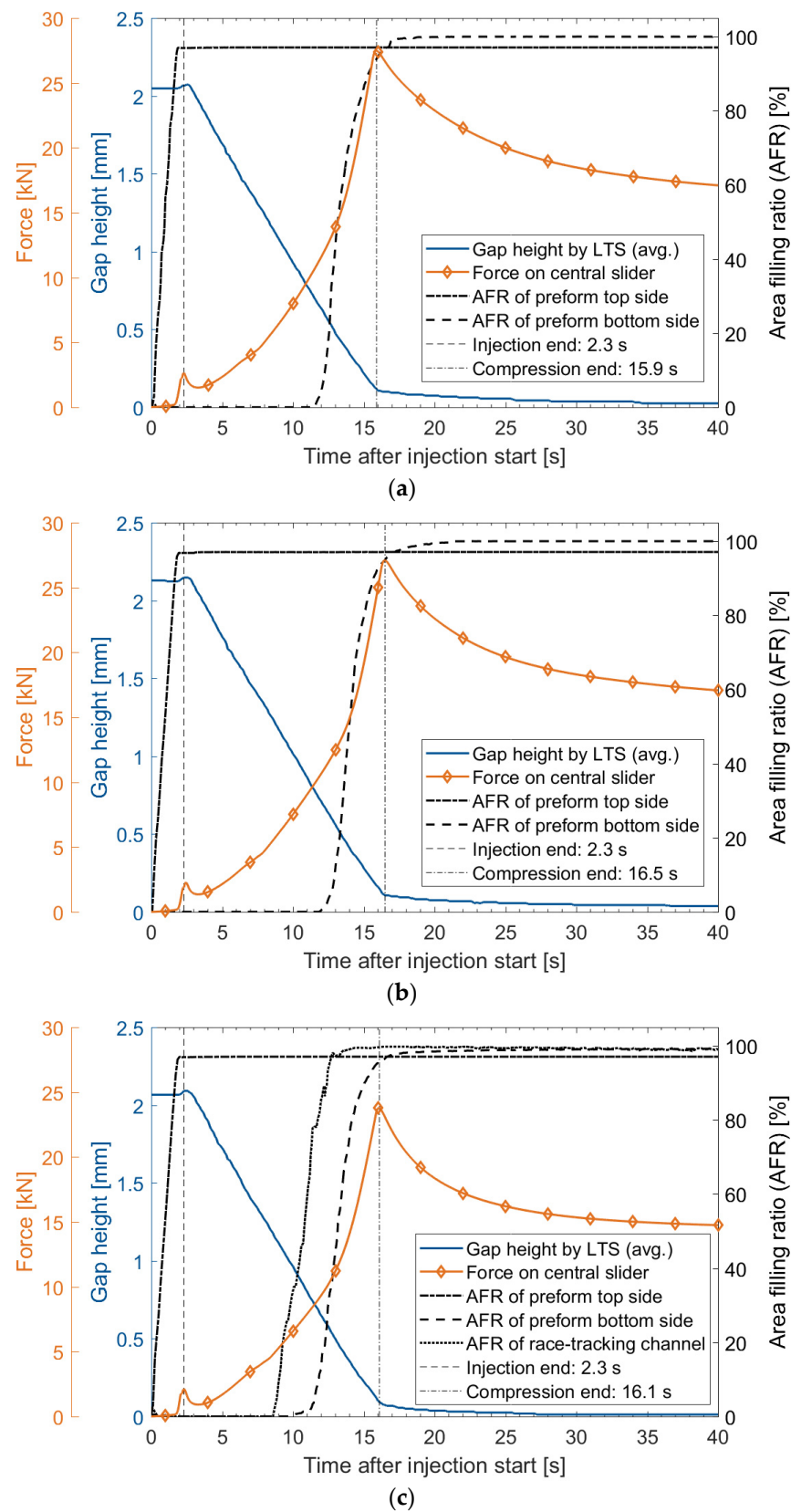


Figure A7. Overview of important process variables during FS-CRTM experiments of the flow control study: (a) no race-tracking channel—fcs-#2; (b) no race-tracking channel—fcs-#3; (c) medium race-tracking channel width—fcs-mrt-#1 (LTS = laser triangulation sensor).

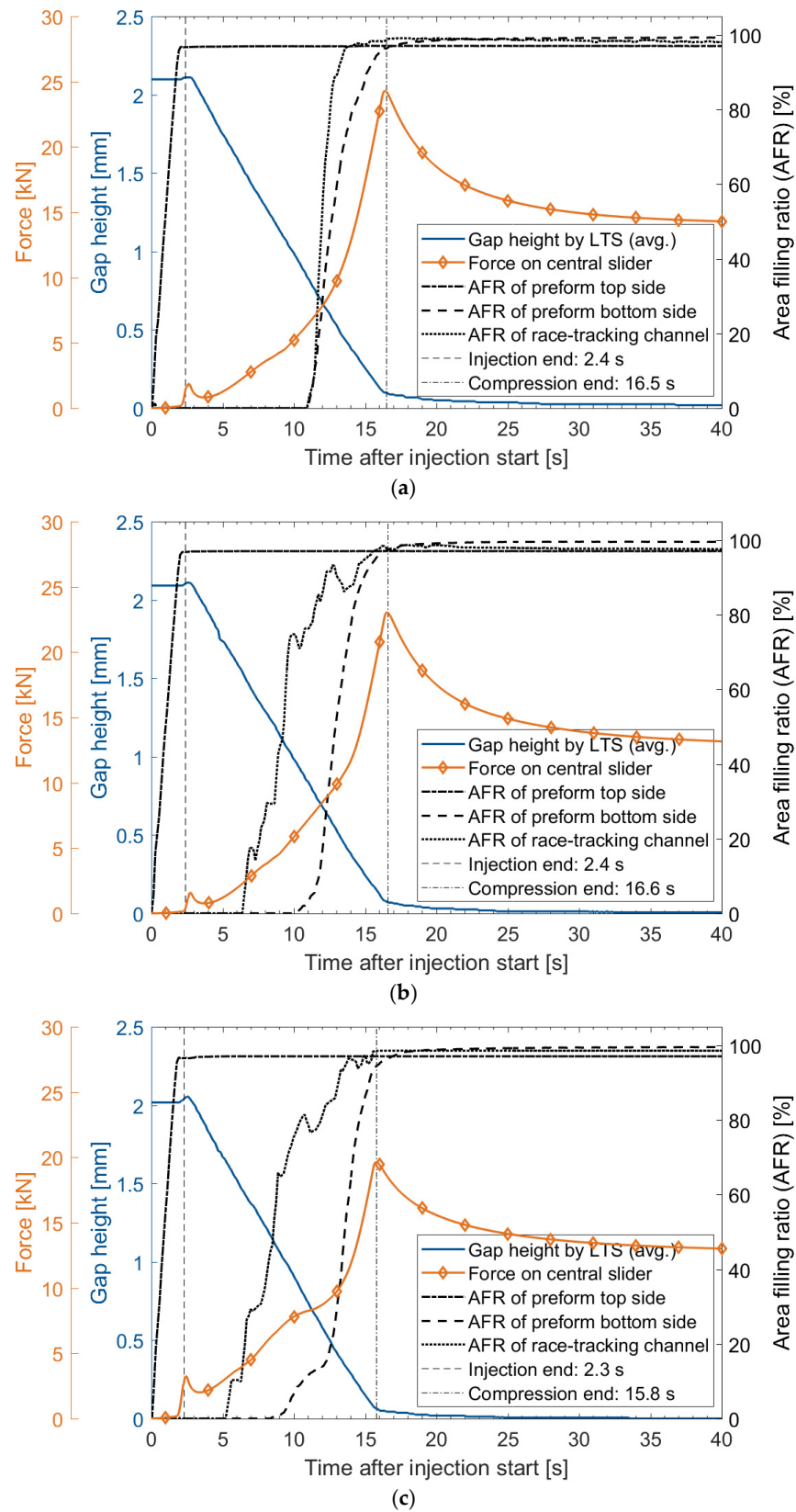


Figure A8. Overview of important process variables during FS-CRTM experiments of the flow control study: (a) medium race-tracking channel width—fcs-mrt-#2; (b) wide race-tracking channel width—fcs-wrt-#1; (c) wide race-tracking channel width—fcs-wrt-#3 (LTS = laser triangulation sensor).

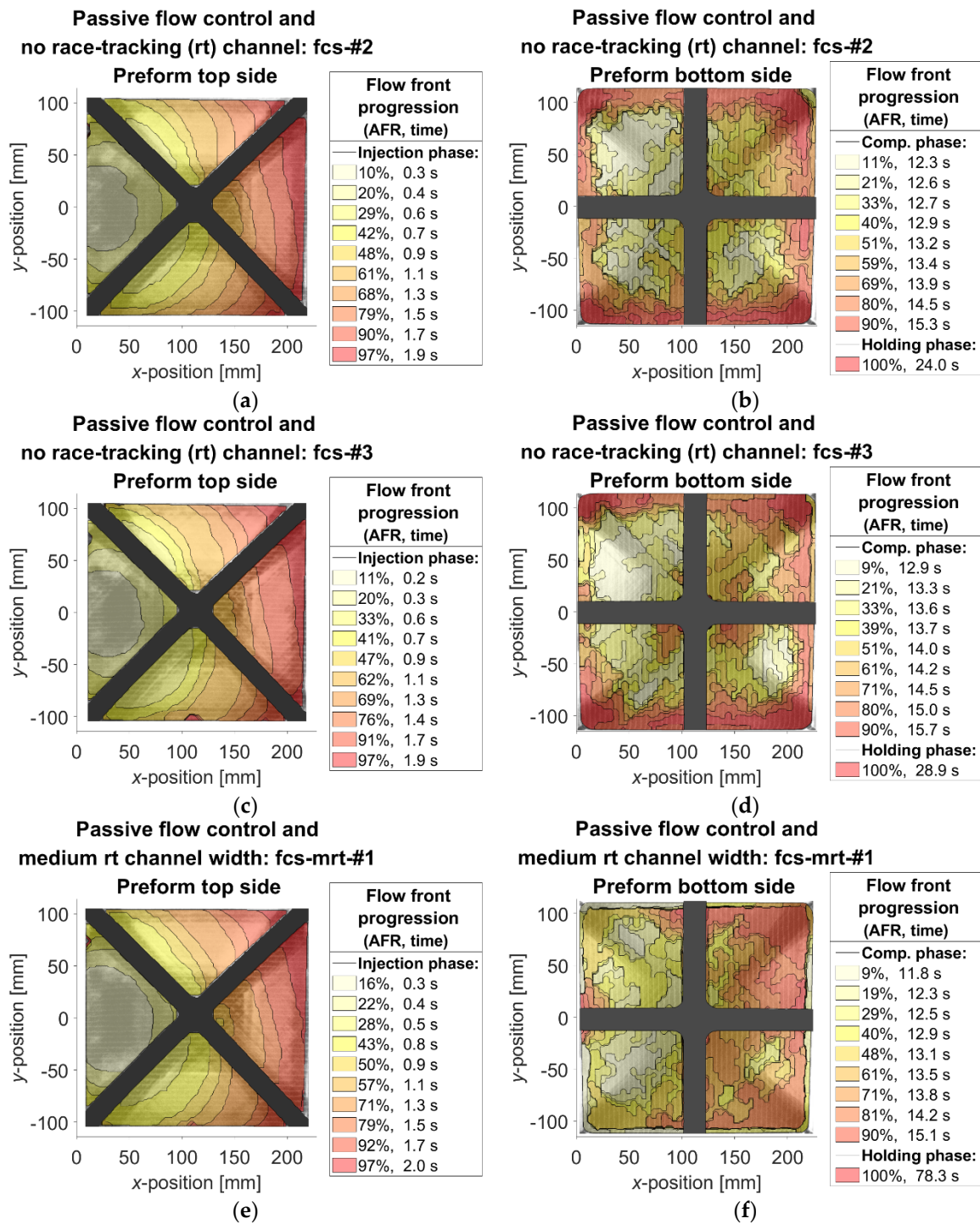


Figure A9. Flow front progression of FS-CRTM experiments of the flow control study: (a,b) no race-tracking (rt) channel—fcs-#2; (c,d) no race-tracking channel—fcs-#3; (e,f) medium race-tracking channel width—fcs-mrt-#1 (AFR = area filling ratio).

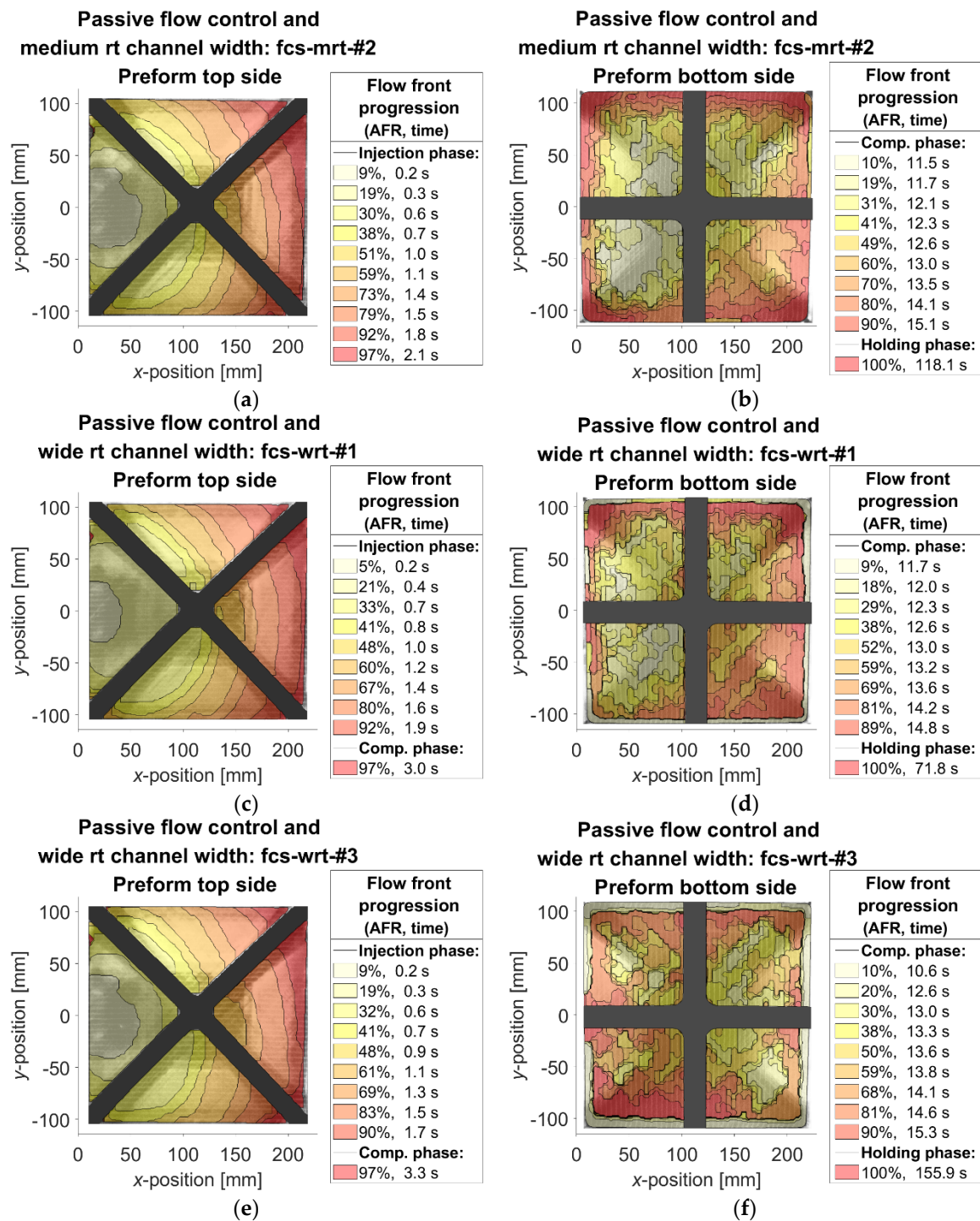


Figure A10. Flow front progression of FS-CRTM experiments of the flow control study: (a,b) medium race-tracking (rt) channel width—fcs-mrt-#2; (c,d) wide race-tracking channel width—fcs-wrt-#1; (e,f) wide race-tracking channel width—fcs-wrt-#3 (AFR = area filling ratio).

References

1. Starke, J. Carbon Composites in Automotive Structural Applications. In Proceeding of the EuCIA: Composites and Sustainability, Brussels, Belgium, 19 March 2016.
2. Deinzer, G. Leichtbau—Anforderungen und Potenziale aus Sicht der Automobilindustrie. In Proceedings of the Hybridica, Munich, Germany, 9 November 2010.
3. Deinzer, G.; Kothmann, M.H.; Roquette, D.; Diebold, F. Audi Ultra-RTM: A Technology for High Performance and Cost Effective CRFP Parts for High Volume Production. In Proceedings of the 17th European Conference on Composite Materials (ECCM17), Munich, Germany, 26–30 June 2016.

4. Roquette, D.; Meyer, F.; Herbeck, L. High Volume Manufacturing of Carbon Fiber Reinforced Plastics for Body in White. Available online: http://voith.com/composites-en/20170516_Bad-Nauheim_Audi_Voith_Online.pdf (accessed on 26 March 2018).
5. Koch, C. Eigenschaftsprofil von Carbonfasergelegen und Deren Wirkzusammenhänge in der Automobilen Großserienproduktion. Ph.D. Thesis, Technical University of Munich, Munich, Germany, 2020.
6. Advani, S.G.; Hsiao, K.-T. (Eds.) Chapter 11: Compression Resin Transfer Moulding (CRTM) in Polymer Matrix Composites. In *Manufacturing Techniques for Polymer Matrix Composites (PMCs)*; Advani, S.G.; Hsiao, K.-T. (Eds.) Woodhead Publishing Limited: Cambridge, UK, 2012; ISBN 9780857090676.
7. Merotte, J.; Simacek, P.; Advani, S.G. Resin Flow Analysis with Fiber Preform Deformation in through Thickness Direction during Compression Resin Transfer Molding. *Compos. Part A Appl. Sci. Manuf.* **2010**, *41*, 881–887. [[CrossRef](#)]
8. Merotte, J.; Simacek, P.; Advani, S.G. Flow Analysis during Compression of Partially Impregnated Fiber Preform under Controlled Force. *Compos. Sci. Technol.* **2010**, *70*, 725–733. [[CrossRef](#)]
9. Simacek, P.; Advani, S.G.; Iobst, S.A. Modeling Flow in Compression Resin Transfer Molding for Manufacturing of Complex Lightweight High-Performance Automotive Parts. *J. Compos. Mater.* **2008**, *42*, 2523–2545. [[CrossRef](#)]
10. Vollmer, M.; Zaremba, S. Enhancing Composite Production by Integrating Thermoplastic Films in Closed Mold LCM Processes. In Proceedings of the 1. RTM Anwenderforum (AVK), Augsburg, Germany, 25 June 2019.
11. Bruckbauer, P. Struktur-Eigenschafts-Beziehungen von Interphasen Zwischen Epoxidharz und Thermoplastischen Funktionschichten für Faserverbundwerkstoffe. Ph.D. Thesis, Technical University of Munich, Munich, Germany, 2018.
12. Advani, S.G.; Sozer, E.M. *Process Modeling in Composites Manufacturing*; Marcel Dekker: New York, NY, USA, 2003; ISBN 0-8247-0860-1.
13. Hammami, A.; Gauvin, R.; Trochu, F.; Touret, O.; Ferland, P. Analysis of the Edge Effect on Flow Patterns in Liquid Composites Molding. *Appl. Compos. Mater.* **1998**, *5*, 161–173. [[CrossRef](#)]
14. Bickerton, S.; Advani, S.G. Characterization and Modeling of Race-tracking in Liquid Composite Molding Processes. *Compos. Sci. Technol.* **1999**, *59*, 2215–2229. [[CrossRef](#)]
15. Han, K.; Lee, L.J. Dry Spot Formation and Changes in Liquid Composite Molding: I-Experimental. *J. Compos. Mater.* **1996**, *30*, 1458–1474. [[CrossRef](#)]
16. Potter, K. *Resin Transfer Moulding*; Chapman & Hall: London, UK, 1997; ISBN 0-412-72570-3.
17. Rudd, C.D.; Kendall, K.N. Towards a Manufacturing Technology for High-Volume Production of Composite Components. *Proc. Inst. Mech. Eng. Part B J. Eng. Manuf.* **1992**, *206*, 77–91. [[CrossRef](#)]
18. Ishii, M.; Mitschang, P.; Weyrauch, F. Verfahren zur Herstellung Faserverstärkter Verbundwerkstoffen. Patent EP000001685947A1, 1 February 2005.
19. Rosenberg, P.; Thoma, B.; Henning, F. Characterization of Epoxy and Poyurethane Resin Systems for Manufacturing of High-Performance Composites in High-Pressure RTM Process. In Proceedings of the 15th Annual SPE Automotive Composites Conference & Exposition (ACCE), Novi, MI, USA, 9 September 2015.
20. Brack, S.; Dauner, W.; Zimmermann, T. Verfahren zum Herstellen eines Faserverstärkten Kunststoffbauteils und Preform für ein Faserverstärktes Kunststoffbauteil. Patent DE102013006770A1, 18 April 2013.
21. Kistner, P.; Könnicke, D.; Diebold, F.; Roquette, D. Verfahren zur Herstellung eines Faserverbundkunststoff-Bauteils. Patent DE102014009408A1, 25 June 2014.
22. Graf, M.; Fürst, T. Verfahren und Anlage zum Herstellen eines Faserverstärkten Kunststoffbauteils. Patent DE102012110353A1, 29 October 2012.
23. Schindelbeck, M. RTM-Verfahren und Dichtungsloses Werkzeug zur Herstellung von Faserverstärkten Kunststoffformteilen. Patent DE102011077468A1, 14 June 2011.
24. Zaremba, S.; Steib, P. Verfahren zur Herstellung eines Bauteils aus einem Faserverbundwerkstoff. Patent WO002015007353A2, 3 June 2014.
25. Guittard, D.; Soro, D.; Poignonec, J.M. Verfahren zur Herstellung eines Gegenstandes aus Verbundwerkstoff durch Transfer-Spritzgießen von Kunstharz (R.T.M.) und Dadurch Hergestellter Gegenstand. Patent DE000069607445T2, 16 December 1996.
26. Rodgers, W.R.; Aitharaju, A.R. Resin Transfer Molding Systems and Control Logic for Manufacturing Fiber-Reinforced Composite Parts. Patent US20200238637A1, 25 January 2019.
27. Kaiser, D. RTM-Verfahren mit Zwischenfaserschicht. Patent DE102014118670A1, 15 December 2014.
28. Kaps, R. Verfahren zur Herstellung eines Faserverbundbauteils. Patent DE102009053549A1, 18 November 2009.
29. Bitterlich, M.; Drechsel, M.; Niederstadt, T. Verfahren und Vorrichtung zum Herstellen eines Faserverbundbauteils und Fahrzeug mit einem Faserverbundbauteil. Patent DE102011112141A1, 1 September 2011.
30. Nielsen, D.R.; Pitchumani, R. Control of Flow in Resin Transfer Molding with Real-Time Preform Permeability Estimation. *Polym. Compos.* **2002**, *23*, 1087–1110. [[CrossRef](#)]
31. Lee, D.H.; Lee, W.I.; Kang, M.K. Analysis and Minimization of Void Formation during Resin Transfer Molding Process. *Compos. Sci. Technol.* **2006**, *66*, 3281–3289. [[CrossRef](#)]
32. Bickerton, S.; Stadtfeld, H.C.; Steiner, K.V.; Advani, S.G. Design and Application of Actively Controlled Injection Schemes for Resin-Transfer Molding. *Compos. Sci. Technol.* **2001**, *61*, 1625–1637. [[CrossRef](#)]

33. Lawrence, J.M.; Hsiao, K.-T.; Don, R.C.; Simacek, P.; Estrada, G.; Sozer, E.M.; Stadtfeld, H.C.; Advani, S.G. An Approach to Couple Mold Design and on-Line Control to Manufacture Complex Composite Parts by Resin Transfer Molding. *Compos. Part A Appl. Sci. Manuf.* **2002**, *33*, 981–990. [[CrossRef](#)]
34. Lawrence, J.M.; Fried, P.; Advani, S.G. Automated Manufacturing Environment to Address Bulk Permeability Variations and Race Tracking in Resin Transfer Molding by Redirecting Flow with Auxiliary Gates. *Compos. Part A Appl. Sci. Manuf.* **2005**, *36*, 1128–1141. [[CrossRef](#)]
35. Hsiao, K.-T.; Advani, S.G. Flow Sensing and Control Strategies to Address Race-Tracking Disturbances in Resin Transfer Molding. Part I: Design and Algorithm Development. *Compos. Part A Appl. Sci. Manuf.* **2004**, *35*, 1149–1159. [[CrossRef](#)]
36. Kang, M.K.; Jung, J.J.; Lee, W.I. Analysis of Resin Transfer Moulding Process with Controlled Multiple Gates Resin Injection. *Compos. Part A Appl. Sci. Manuf.* **2000**, *31*, 407–422. [[CrossRef](#)]
37. Rosenberg, P. Entwicklung einer RTM Prozessvariante zur Kavitätsdruckgeregelten Herstellung von Faserverbundstrukturbauteilen. Ph.D. Thesis, Karlsruhe Institute of Technology (KIT), Karlsruhe, Germany, 2018.
38. Arnold, M.; Medina, L.A.; Mitschang, P. Varietherme Prozesse zur Herstellung von Hochleistungsverbundwerkstoffen. *Lightweight Des.* **2015**, *8*, 58–61. [[CrossRef](#)]
39. Zaremba, S. Bypassströmungen im Füllprozess Textiler Strukturen: Charakterisierung, Abbildung und Optimierung. Ph.D. Thesis, Technical University of Munich, Munich, Germany, 2018.
40. Vollmer, M.; Nusser, F.; Bublitz, D.; Baumann, H.; Graßl, L.; Masseria, F.; Zaremba, S.; Mertiny, P.; Drechsler, K. Increasing Process Robustness of the Compression Resin Transfer Molding Process Towards Edge Race-Tracking. In Proceedings of the SAMPE Europe Conference 2021, Baden, Switzerland, 29 September 2021.
41. Dirschmid, F. Die CFK-Karosserie des BMW i8 und deren Auslegung. In *Karosseriebautage Hamburg: 13. ATZ-Fachtagung*; Tecklenburg, G., Ed.; Springer Fachmedien Wiesbaden: Wiesbaden, Germany, 2014; pp. 217–231. ISBN 978-3-658-05980-4.
42. Tecklenburg, G.; Ahlers, M. Carbon Core: Die neue BMW 7er Karosserie. In *Karosseriebautage Hamburg 2016*; Springer Vieweg: Berlin, Germany, 2016; pp. 125–135. [[CrossRef](#)]
43. Lomov, S.V. *Non-Crimp Fabric Composites: Manufacturing, Properties and Applications*; Woodhead Publishing Limited: Cambridge, UK, 2011; ISBN 978-0-85709-253-3.
44. SGL Group. *Data Sheet: SIGRATEx C B310-45/ST-E214/5g—Stitched, Biaxial, Carbon Fiber Fabric with Powder Binder*; SGL Group: Wiesbaden, Germany, 2017.
45. Vollmer, M.; König, D.; Gilch, I.; Waller-Ehret, H.; Zaremba, S.; Hübner, C.; Mertiny, P.; Drechsler, K. Identification of a Film to Seal the Preform Impregnation during the Compression Resin Transfer Molding Process. In Proceedings of the SAMPE Europe Conference 2021, Baden, Switzerland, 29 September 2021.
46. Rosenberg, P.; Thoma, B.; Henning, F. Investigation and Validation of a new Cavity Pressure Controlled HP-RTM Process Variant (PC-RTM). In Proceedings of the 16th Annual SPE Automotive Composites Conference & Exposition (ACCE), Novi, MI, USA, 7 September 2016.
47. Solvay. *Data Sheet: Flashtape1, Adhesive Tape*; Solvay: Alpharetta, GA, USA, 2019.
48. Richmond Aerovac. *Data Sheet: Raphold 1, High Temperature Double Backed Tape*; Richmond Aerovac: Richmond, CA, USA, 2010.
49. Richmond Aerovac. *Data Sheet: LTS90B/G, Sealant Tape*; Richmond Aerovac: Richmond, CA, USA, 2010.
50. Richardson, M.O.W.; Zhang, Z.Y. Experimental investigation and flow visualisation of the resin transfer mould filling process for non-woven hemp reinforced phenolic composites. *Compos. Part A Appl. Sci. Manuf.* **2000**, *31*, 1303–1310. [[CrossRef](#)]
51. Terzaghi, K. *Theoretical Soil Mechanics*; John Wiley and Sons, Inc.: New York, NY, USA; London, UK, 1943.
52. Li, L.; Zhao, Y.; Yang, J.; Zhang, J.; Duan, Y. An experimental investigation of compaction behavior of carbon non-crimp fabrics for liquid composite molding. *J. Mater. Sci.* **2015**, *50*, 2960–2972. [[CrossRef](#)]